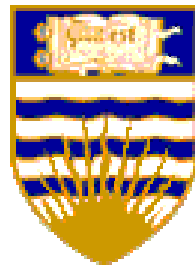


Resonant Soft X ray scattering

George Sawatzky

University of British Columbia

Vancouver BC Canada



Collaborators

Scattering:

P.Abbamonte, J.Hill, J. Thomas ---- BNL

L Venema, A.Rusydi, ----- Groningen

D. Feng, A. Damascelli, I. Elfimov----UBC

E.Isaacs, G.Bloomberg, A. Gozar ----- Bell

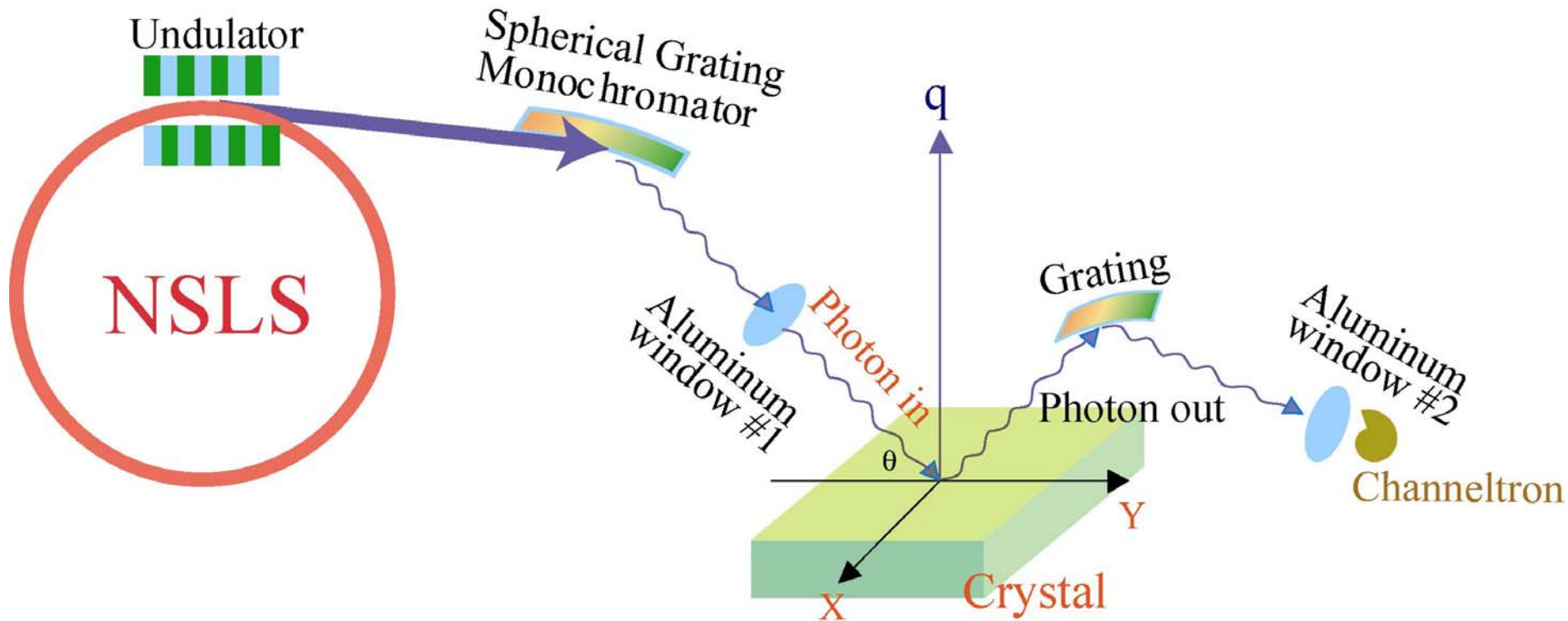
Samples:

I.Bozovic ----- BNL

D.Bonn, W.Hardy, R.Z.Liang --- UBC

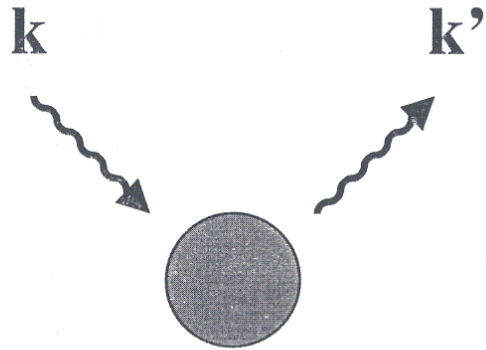
H.Eisaki, S.Uchida ---- Tokyo

Experimental Setup



- NSLS, undulator beamline X1B, photon energy: 85~1800 eV
- about $5 \cdot 10^{12}$ photon/sec at a typical 1000 resolving power
- Removable Aluminum windows to block low energy stray light
- XAS taken in Fluorescence/Electron yield modes
- Removable 2nd grating to select the primary energy
- 2.4 m sized UHV chamber, 10 motions, T=30~400K

X-ray Scattering

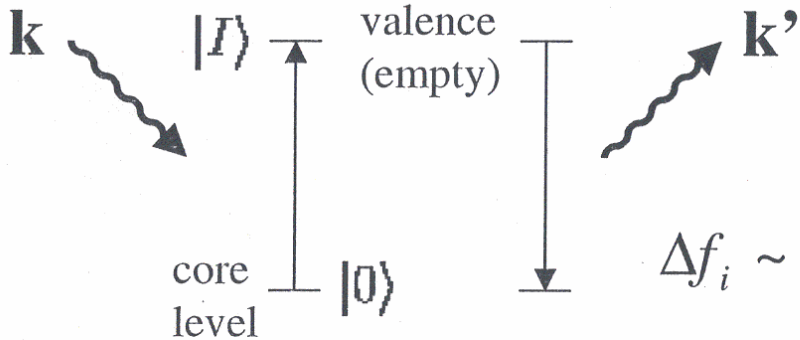


$$\mathbf{G} = \mathbf{k}' - \mathbf{k}$$

$$f_i^0 = 4\pi \int dr n_i(r) r^2 \frac{\sin(\vec{G} \cdot \vec{r})}{|\vec{G} \cdot \vec{r}|}$$

└─ electron number density

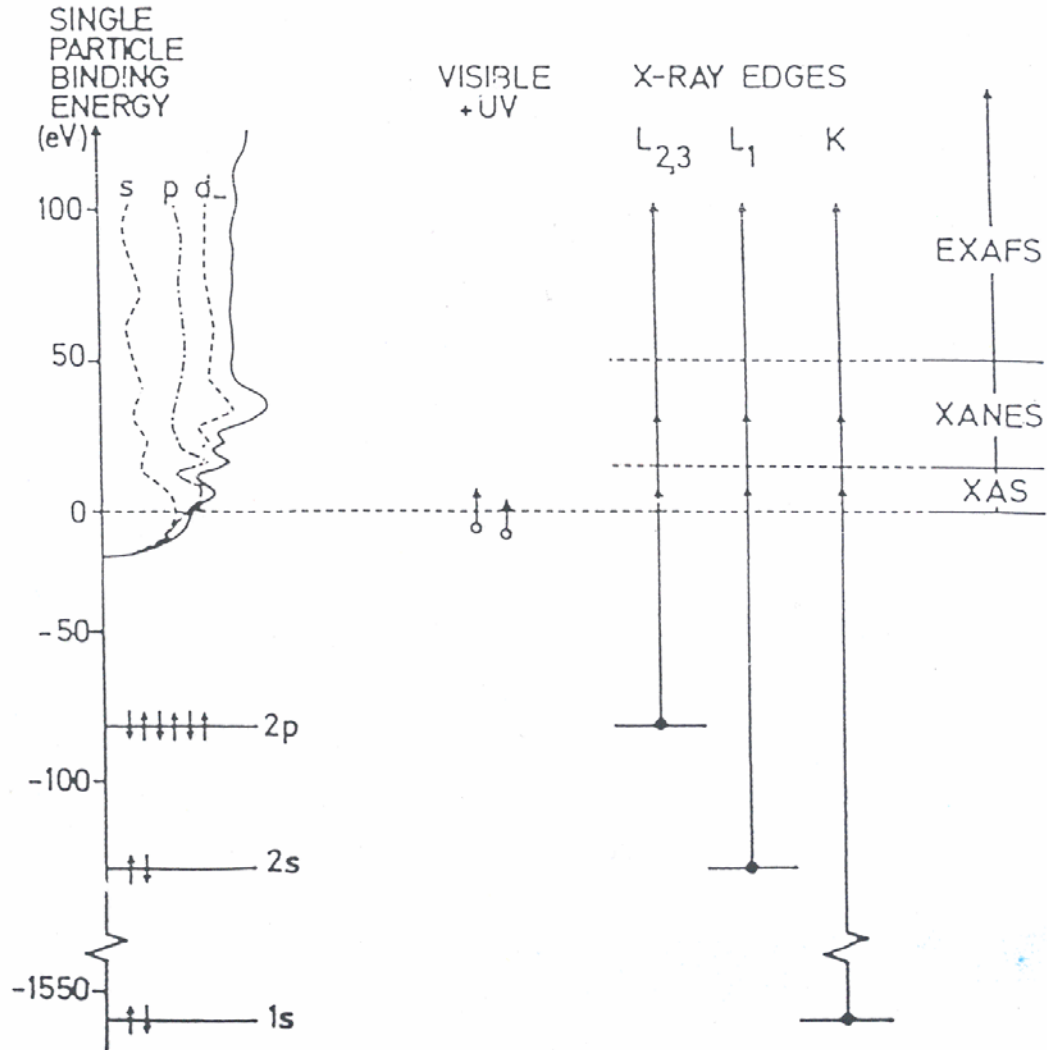
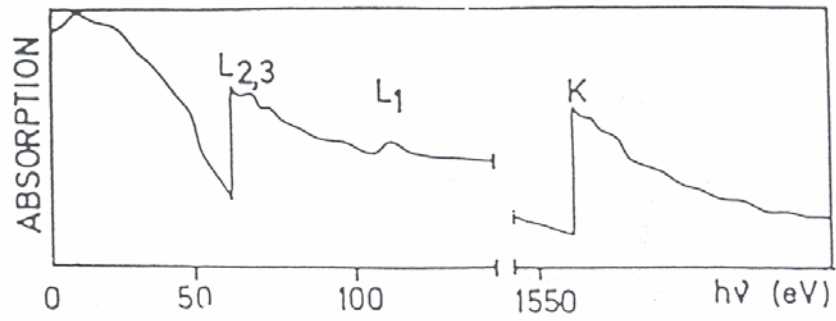
Resonant X-ray Scattering



$$\Delta f_i \sim \sum_I \frac{\langle 0 | \vec{\epsilon} \cdot \vec{r} \exp(i\vec{k} \cdot \vec{r}) | I \rangle \langle I | \vec{\epsilon}' \cdot \vec{r} \exp(i\vec{k}' \cdot \vec{r}) | 0 \rangle}{\hbar\omega - (E_I - E_0) - i\Gamma}$$

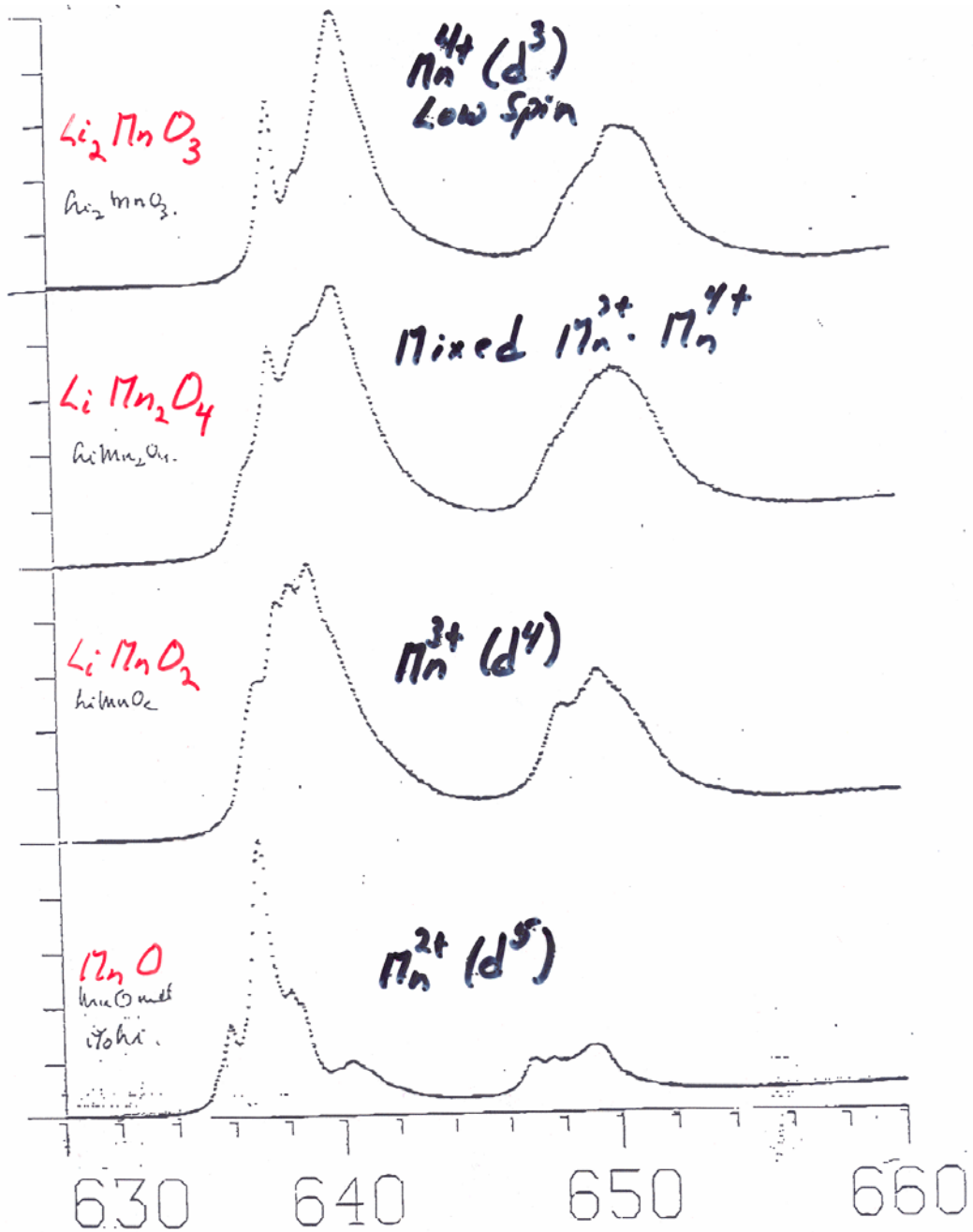
We learn about the spatial distribution of states $|I\rangle$

Enhancement at resonance 3-4 orders of magnitude



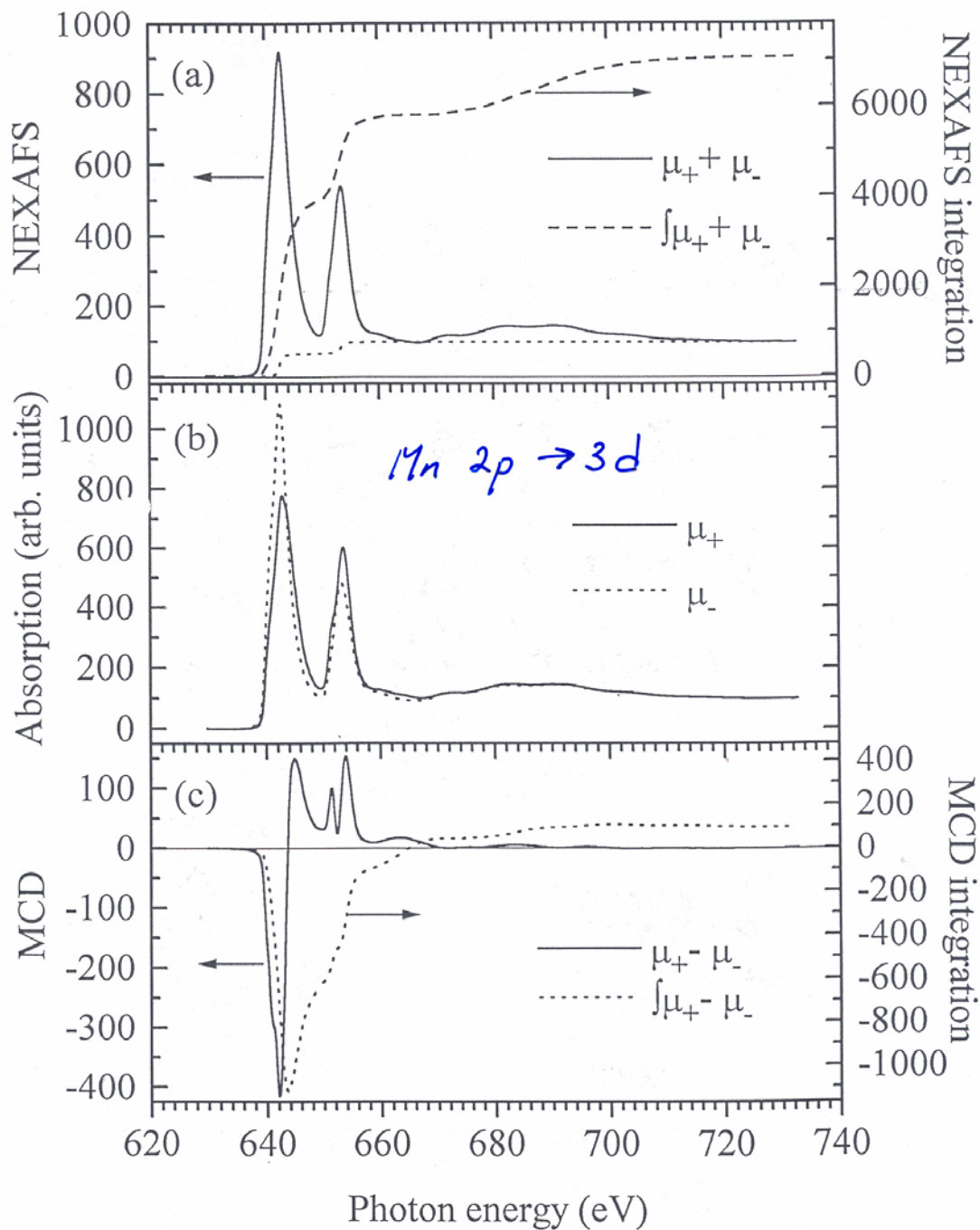
At resonance we have contrast for:

- Elements
- Valence electron density
- Bond orientation; orbital ordering
quadrupole moment orientation
[linear pol. light]
- Spin density [circular pol. light and
p or *d* core level]





Pellegrin et al.



Modern materials research

- Small crystals
- (ultra) thin films [few atoms]
- Multilayers
- Nano structures
- self assembled systems
- Atoms and molecules on surfaces

Reminder

$$\lambda = \frac{E}{12000 \text{ eV}} \text{ \AA}$$

3d Transition Metal Compounds

$L_{2,3}$ edge $2p \rightarrow 3d$

500 eV \rightarrow 900 eV

20 \AA \rightarrow 12 \AA

Rare Earth's (4f compounds)

$M_{4,5}$ edge $3d \rightarrow 4f$

800 eV \rightarrow 1800 eV

12 \AA \rightarrow 8 \AA

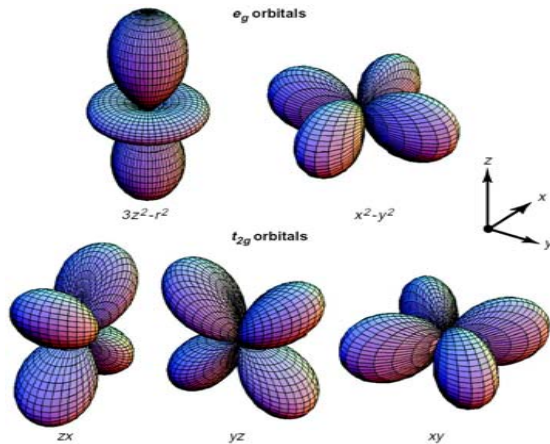
C_{1s} - 280 eV \rightarrow 40 \AA

N_{1s} - 390 eV \rightarrow 35 \AA

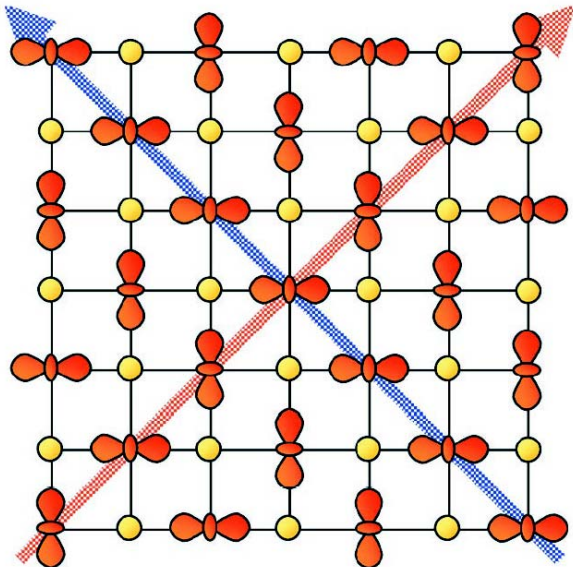
O_{1s} - 530 eV \rightarrow 25 \AA

S_{1s} - 3000 eV \rightarrow 4 \AA

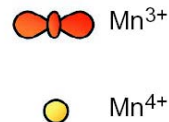
Ordering in strongly correlated systems



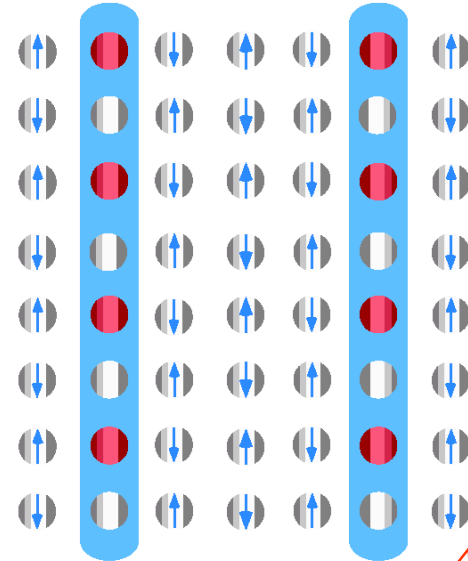
charge/orbital ordering in $\text{La}_{0.5}\text{Sr}_{1.5}\text{MnO}_4$



$\Delta Q_c \sim 1 e$
 $\Delta Q_o \sim 0$



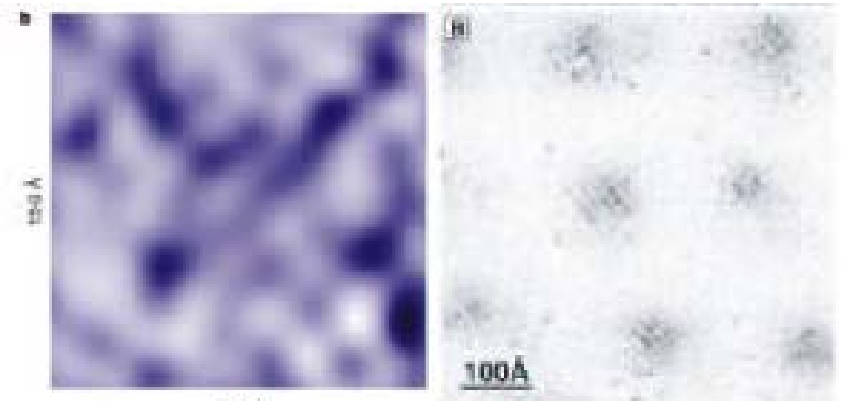
Stripes in Nd-LSCO



$\Delta Q < 0.5 e$

$\Delta Q/Q_{\text{total}} \sim 1/500$

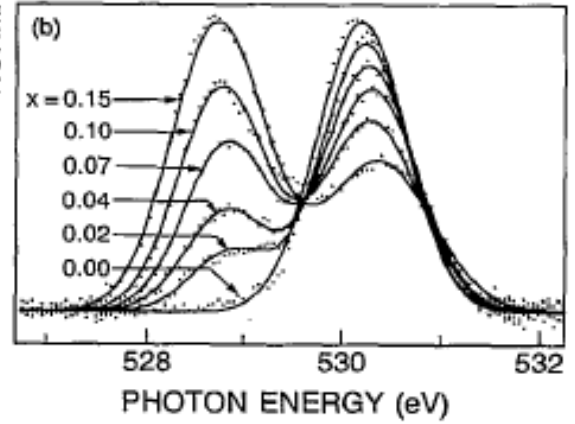
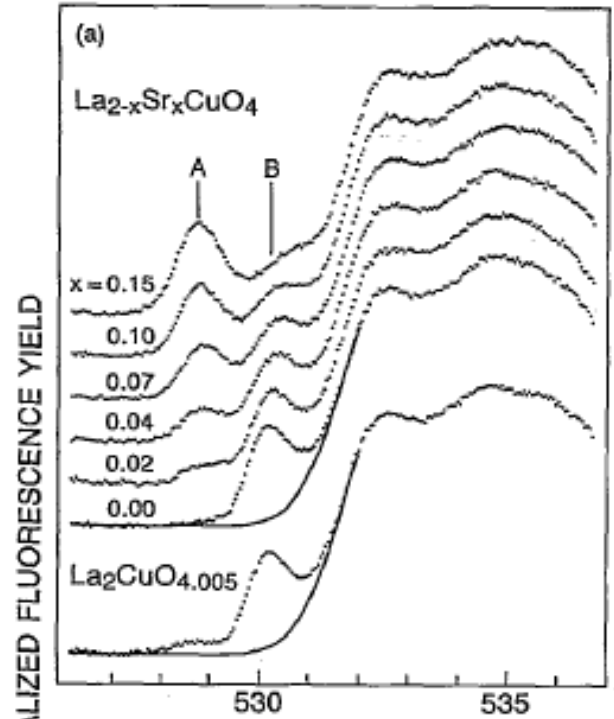
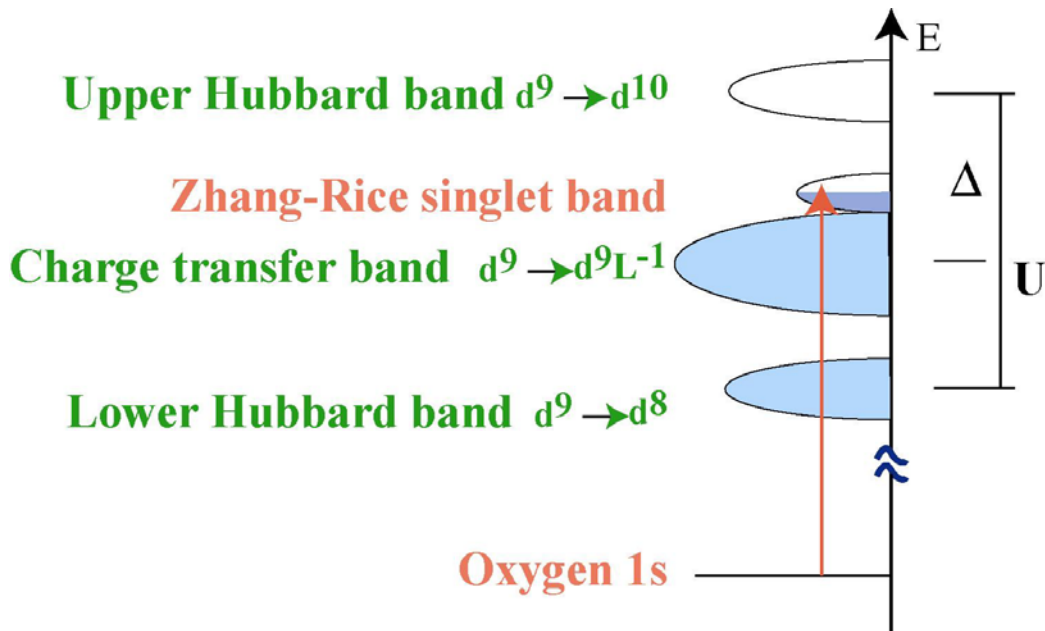
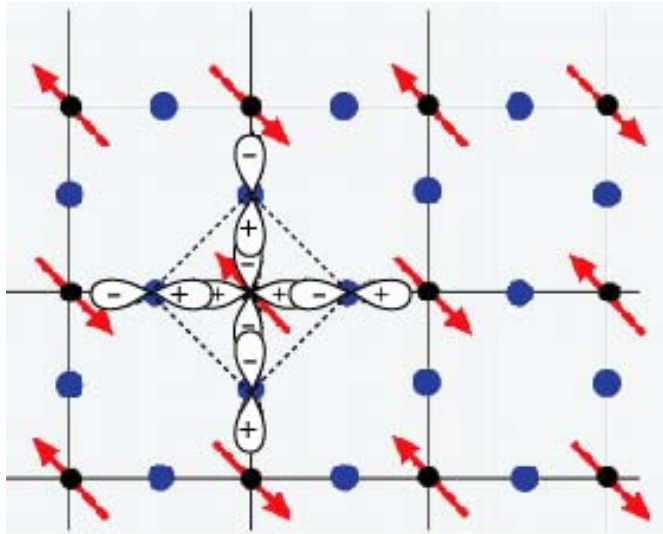
Charge inhomogeneity in Bi2212



Pan, *Nature*, **413**, 282 (2001);
 Hoffman, *Science*, **295**, 466 (2002)

$\Delta Q \sim 0.1 e$

Doped holes in cuprate

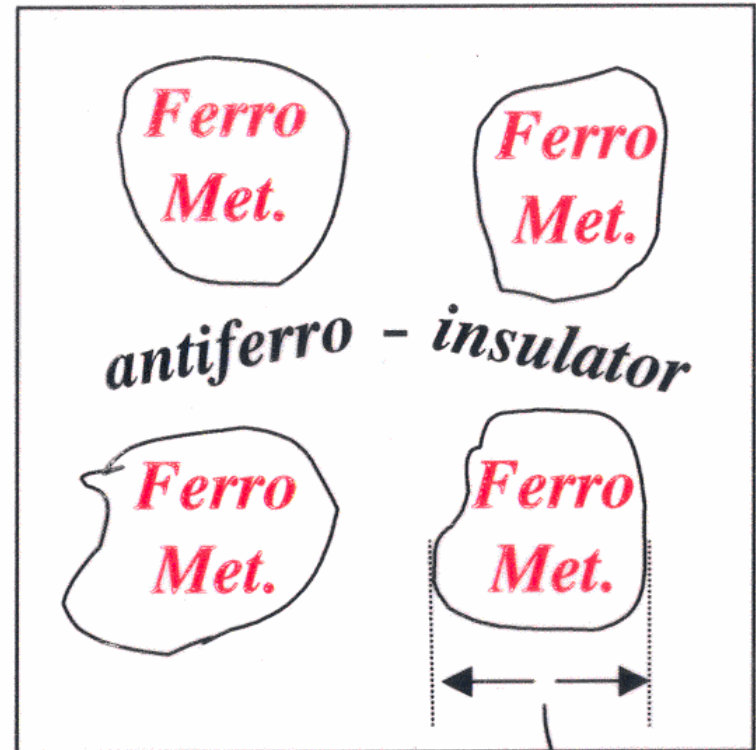


Phase Separation

- Stripes in High T_C 's?
- Magnetic droplets in manganites

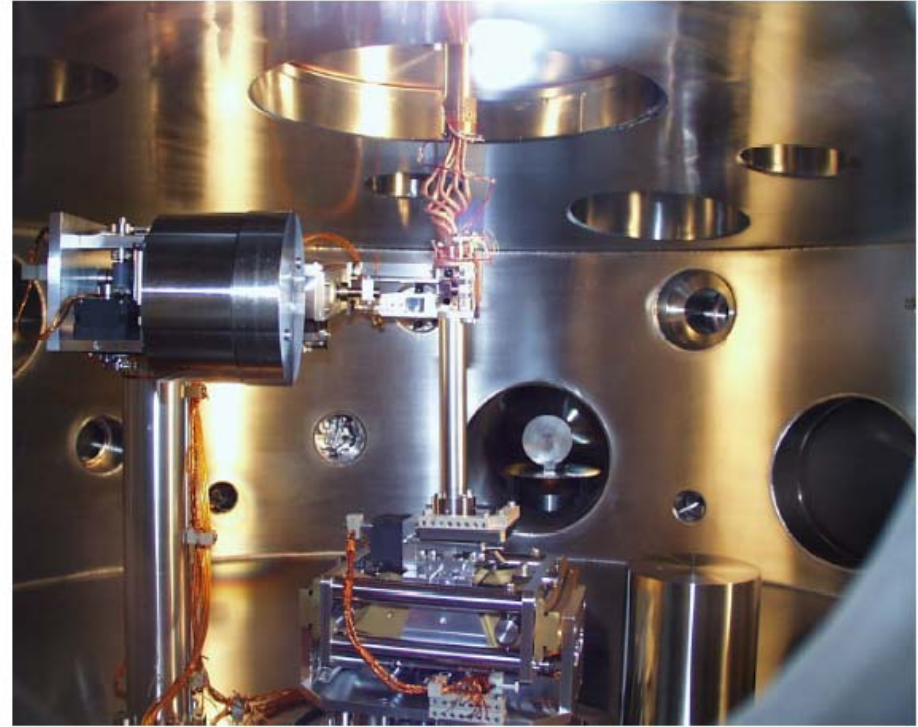
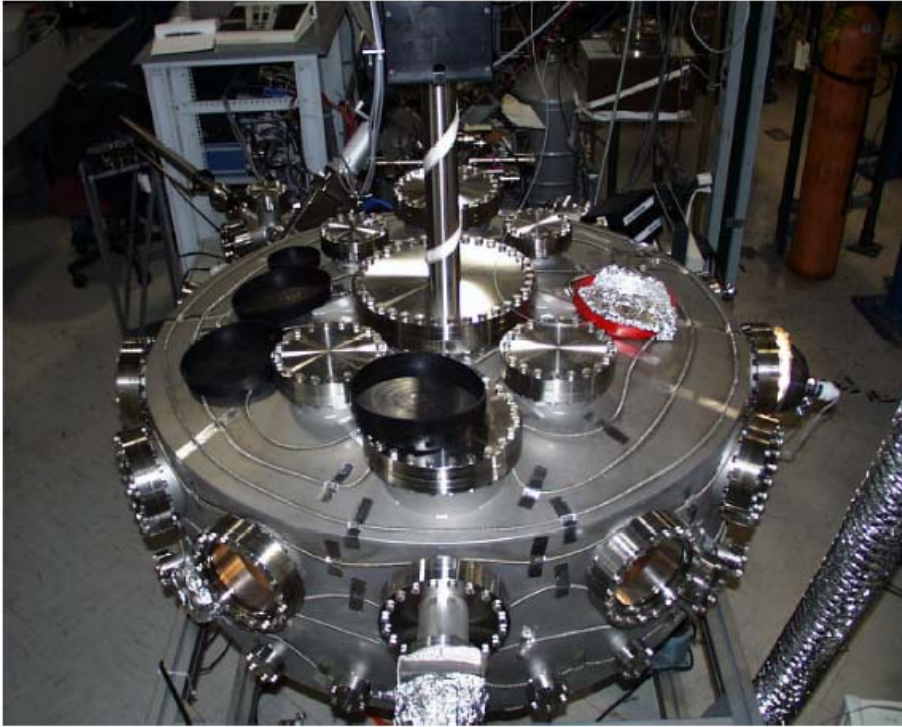
Diffuse Scattering

Exp. at $L_{2,3}$ edge would be much more sensitive than at the K edge



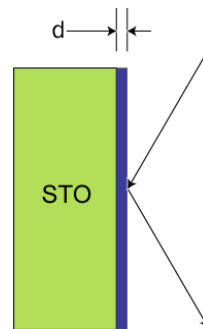
1 - 20 nm

Experimental Station



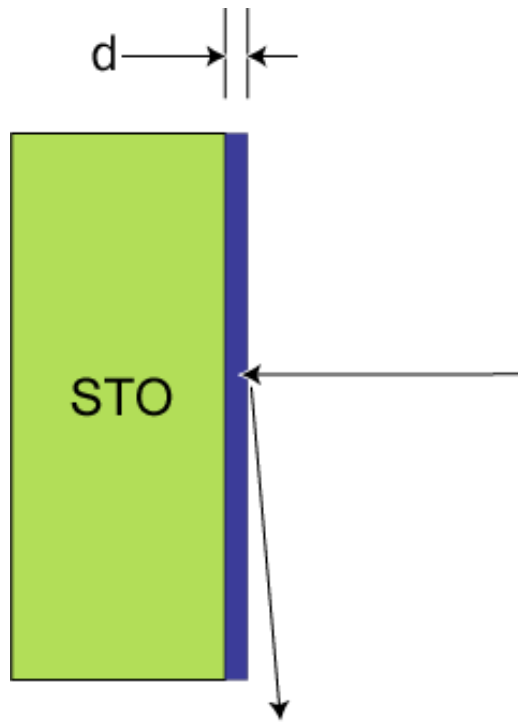
- 2.4m diameter vacuum chamber
- 5 circle geometry (10 motions)
- Integrated beamline + end station control
- Helium flow cryostat (15~400K)
- 5 Tesla magnet (vertical)
- UHV, Base pressure $\sim 10^{-10}$ torr

Sensitivity to holes: Resonant Soft X-ray Fringes of LSCO film



P. Abbamonte *et al.* "A Structural Probe of the Doped Holes in Cuprate Superconductors", *Science*, **297**, 581 (2002)

XAS at Oxygen K and Copper L edge



Epitaxial $\text{La}_2\text{CuO}_{4+\delta}$ on SrTiO_3

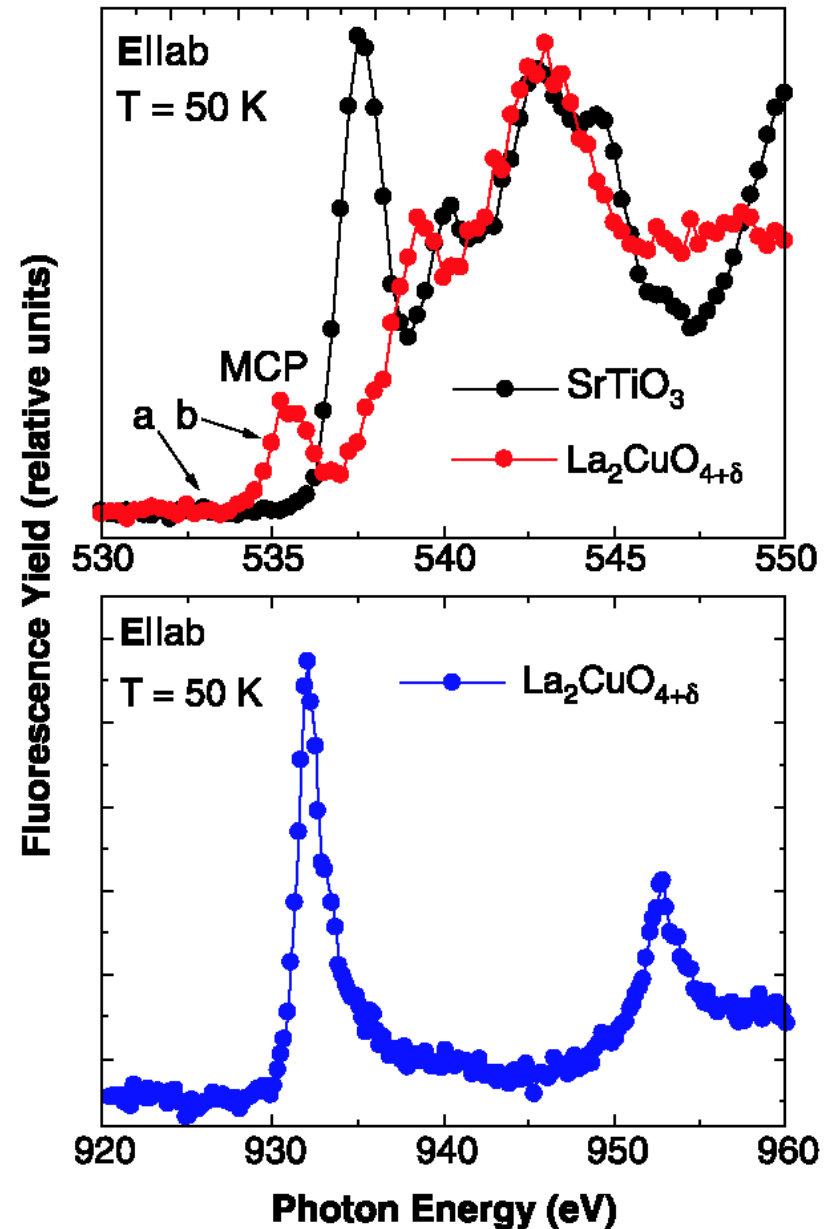
($d = 23.3 \text{ nm}$, $T_c = 39 \text{ K}$)

$$2d \sin(\theta) = n \lambda$$

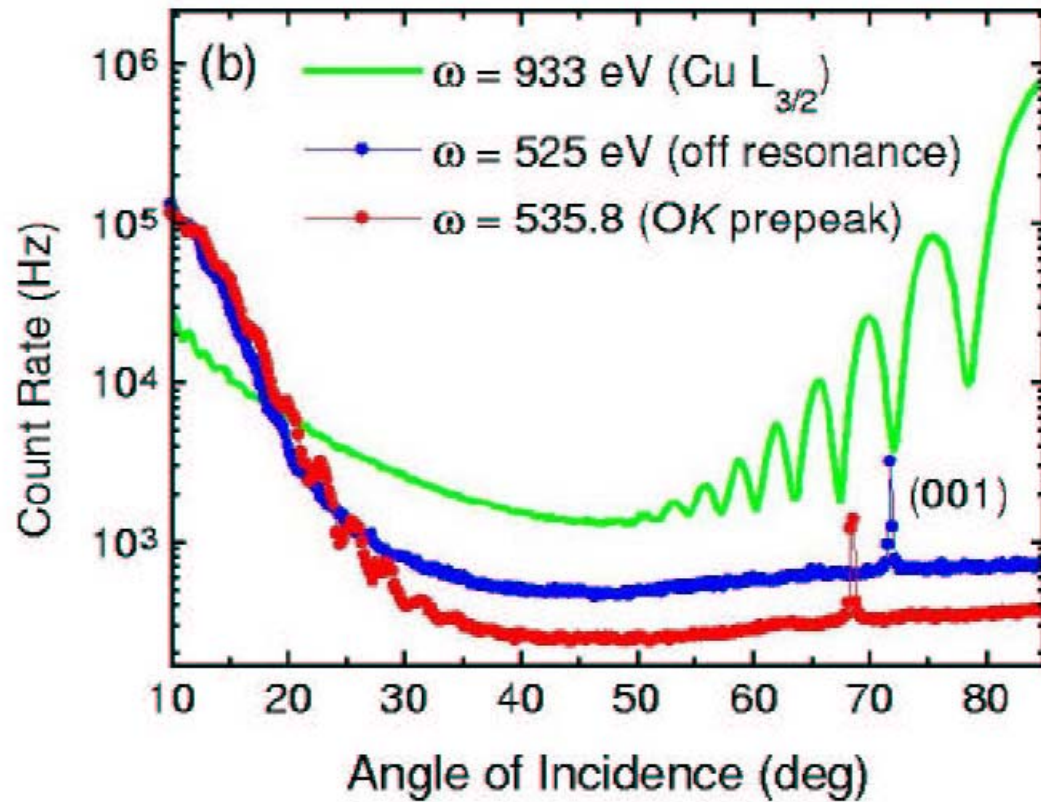
$$n_{\text{STO}} = 5.12 \text{ g/cm}^3$$

$$n_{\text{LSCO}} \sim 5.5 \text{ g/cm}^3$$

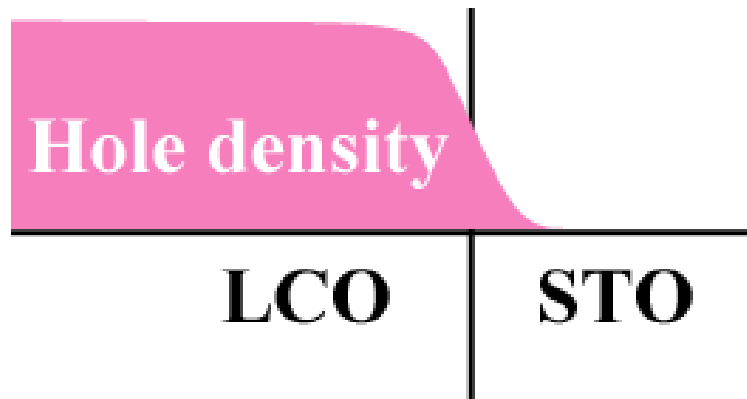
$T = 50 \text{ K}$



Anomaly in Fringe Envelope

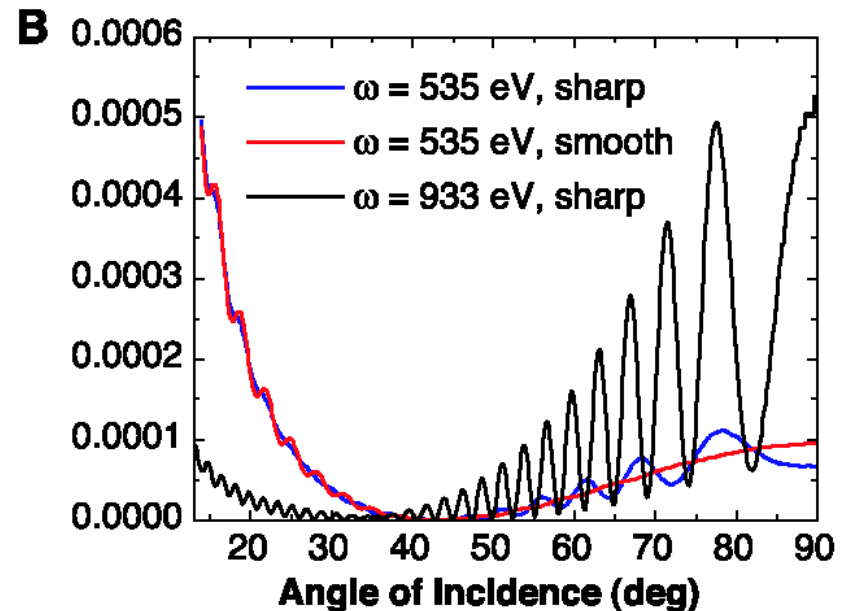
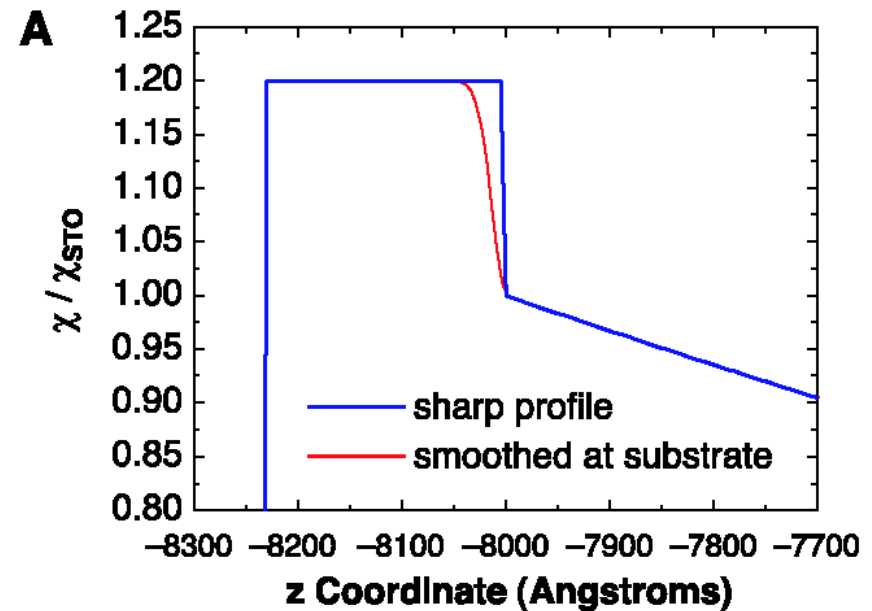


Hole depletion model

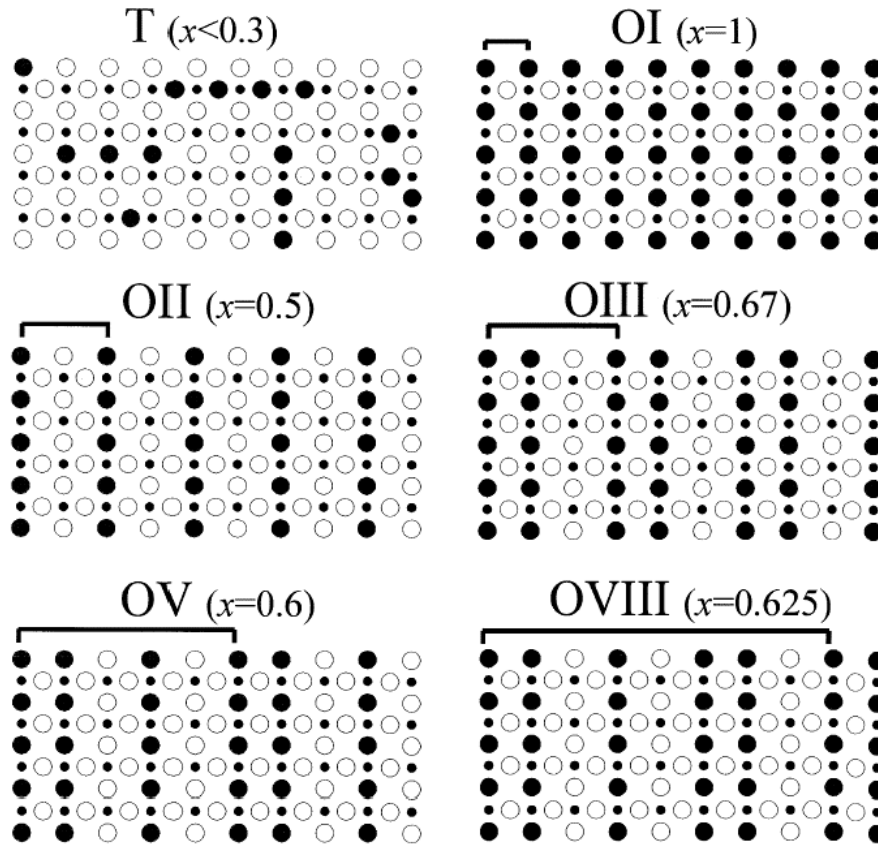


$$\phi_{\text{STO}} = 3.2 \text{ eV Reihl, } PRB \text{ 30, 803 (1984)}$$

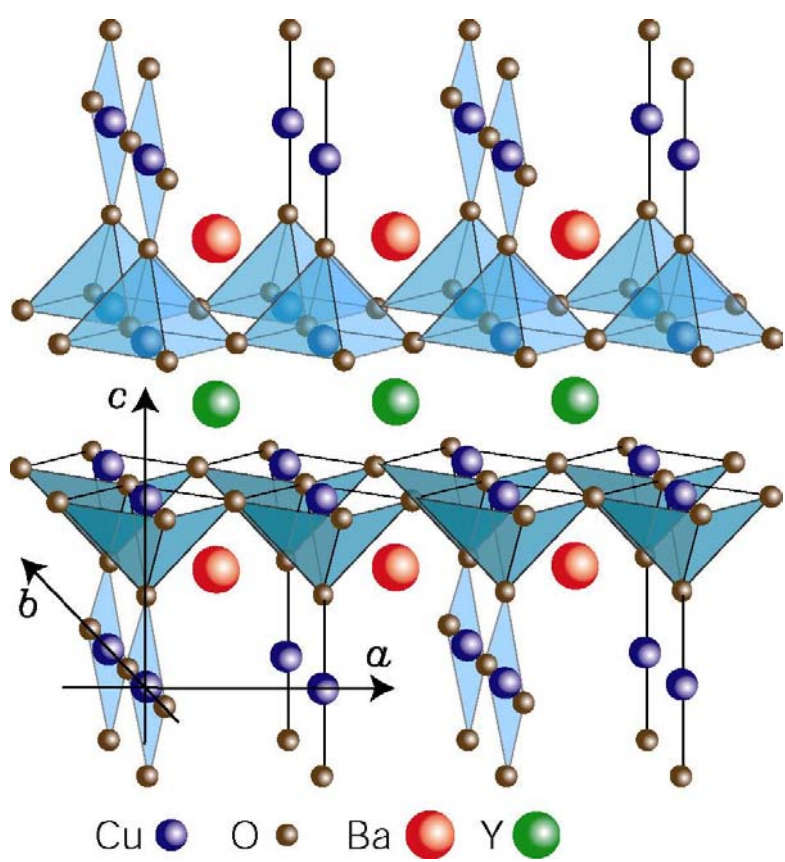
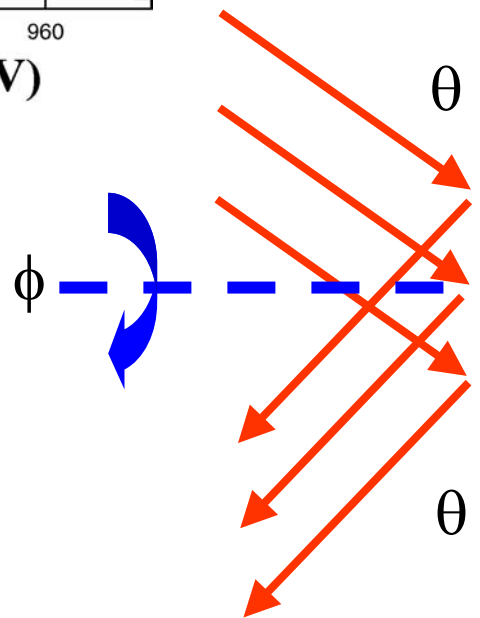
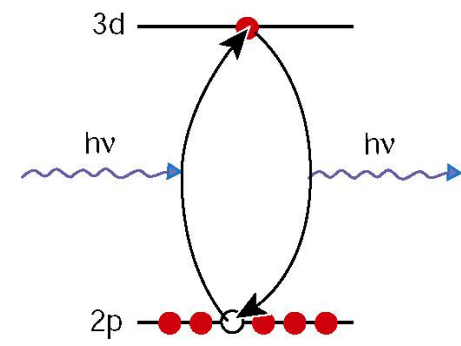
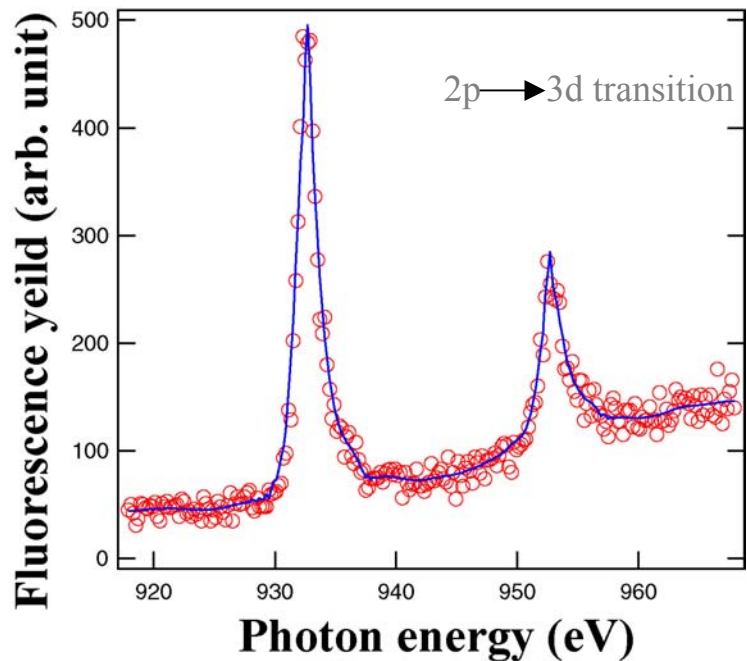
$$\phi_{\text{LSCO}} = 4.7 \text{ eV v. d. Marel, } Physica \text{ C 241,273 (1995)}$$



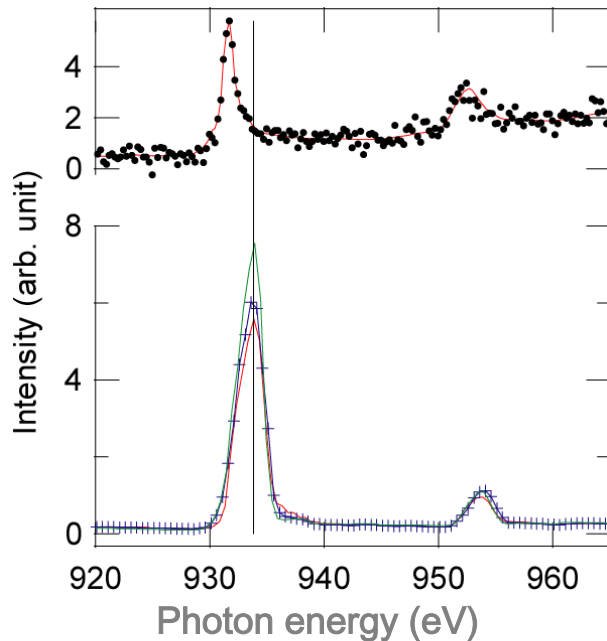
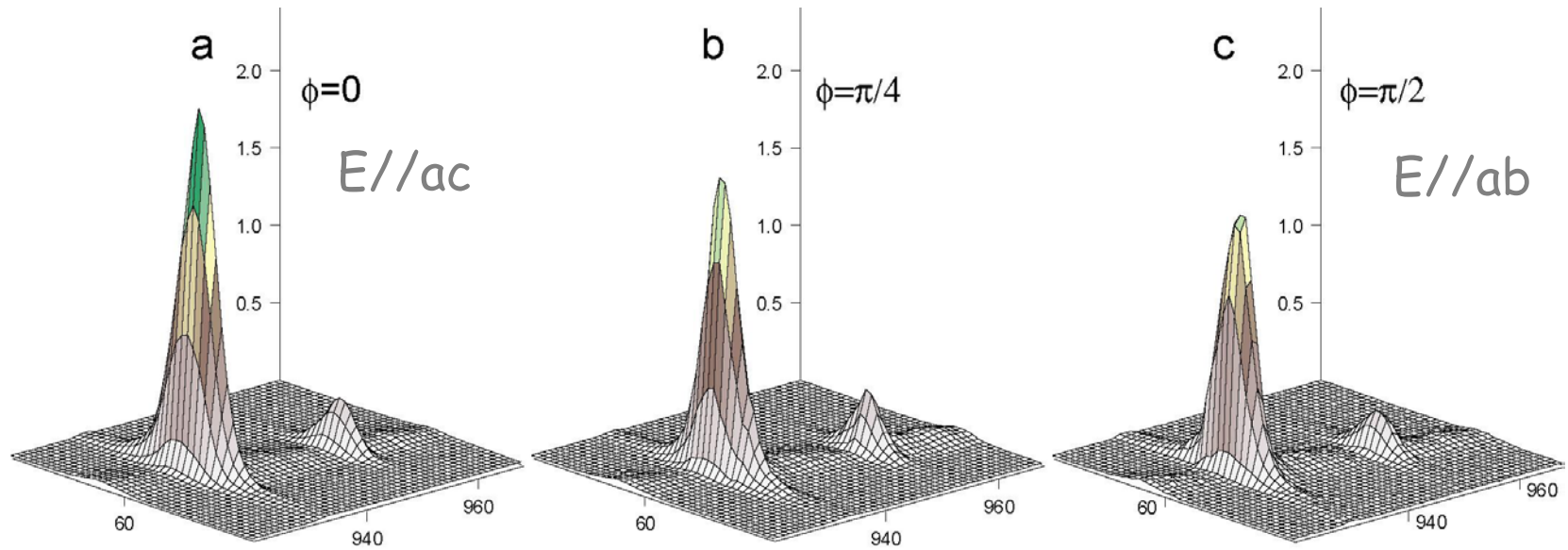
YBCO oxygen ordering



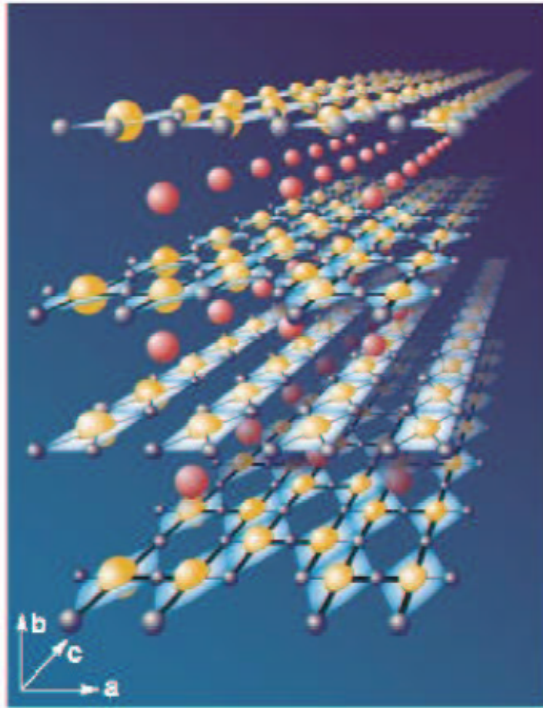
Experimental Geometry



Zooming-in on different Cu's: Tuning Polarization

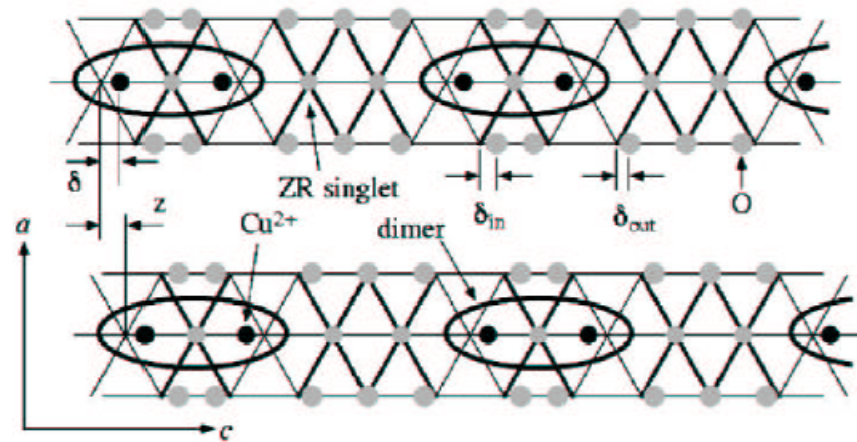


At L_3 edge, $I(E//ac)/I(E//ab) = 1.3$

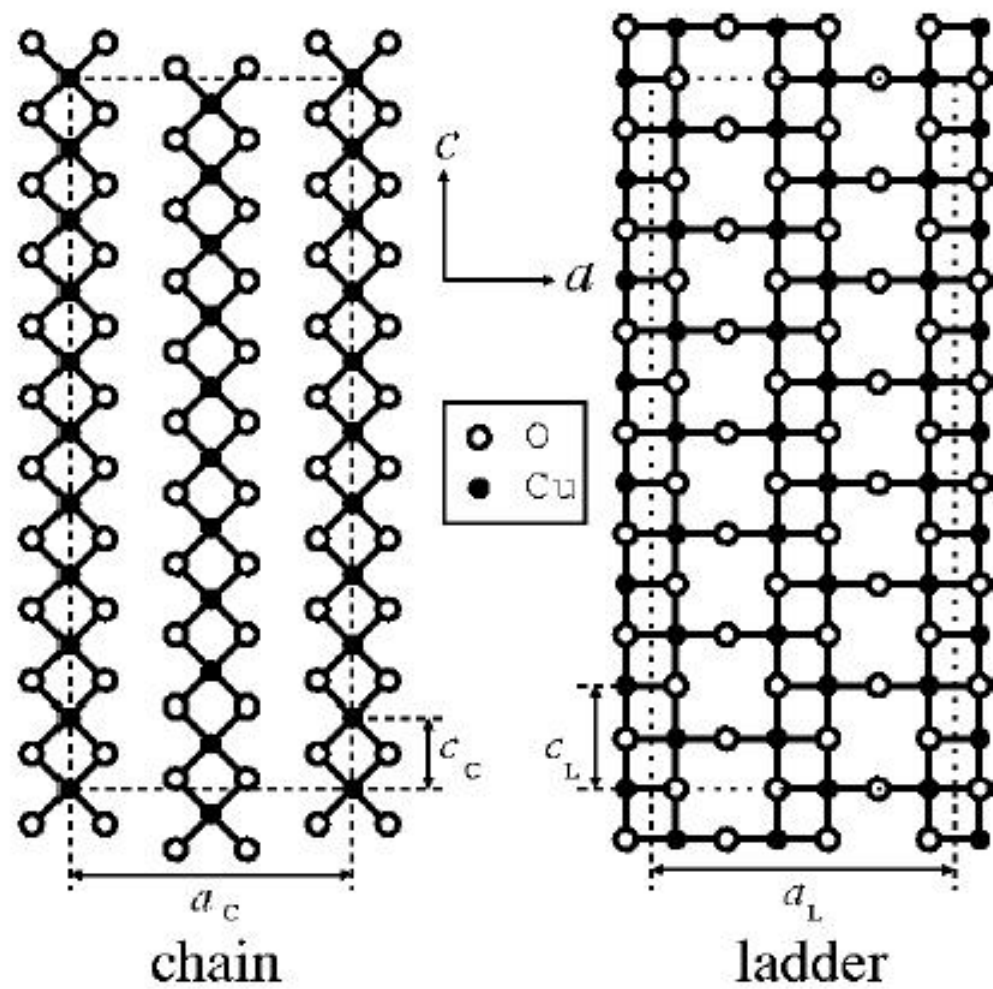
$Sr_{14}Cu_{24}O_{41}$ – “telephone number” material


Girsh, *Science*, **297**, 584 (2002)

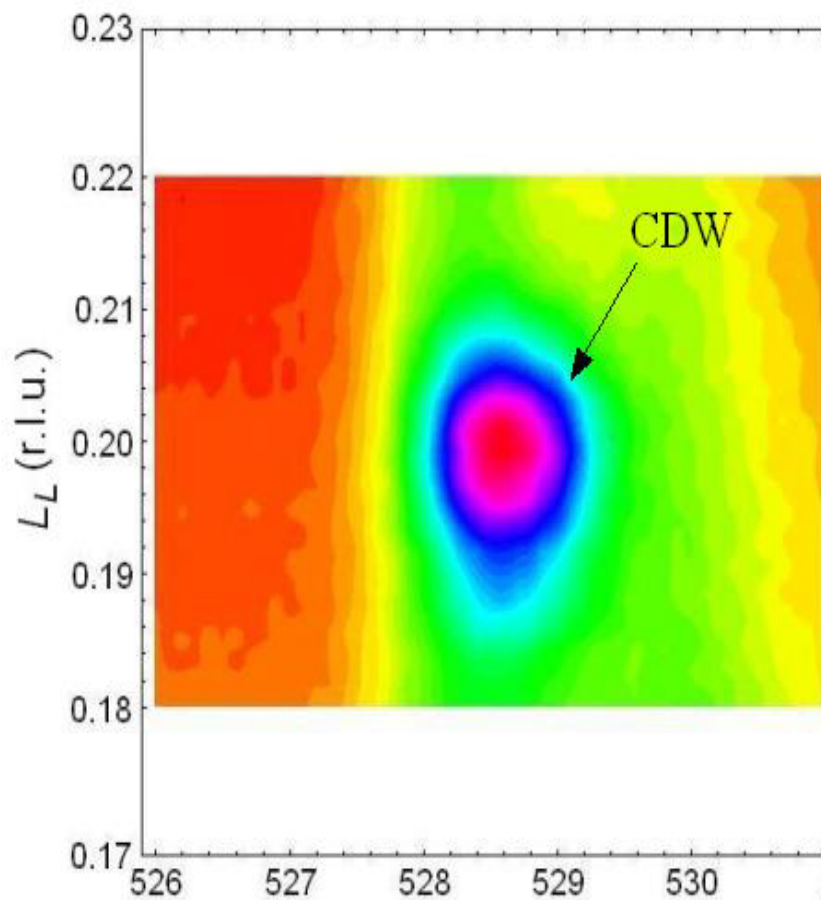
6 holes per unit cell
5 on chains
1 on ladder



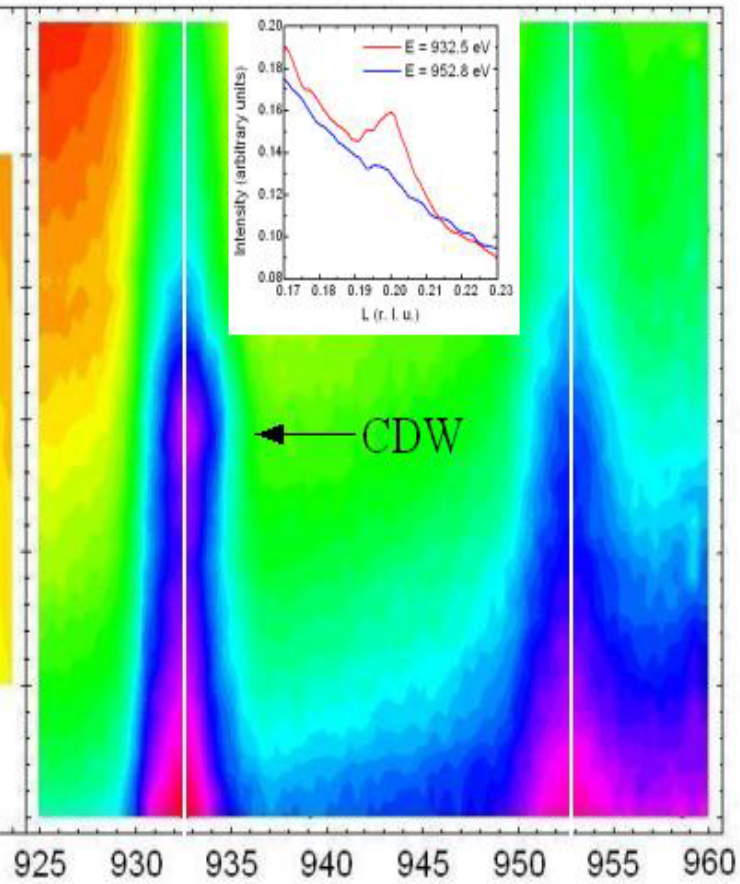
- Dimerized chain, CDW / SDW order
- Ladder $J_{\perp} = J_{\parallel} \Rightarrow$ RVB state with spin gap and *different* CDW / SDW order.
[Gozar, *PRL*, **87**, 197202 (2001)]



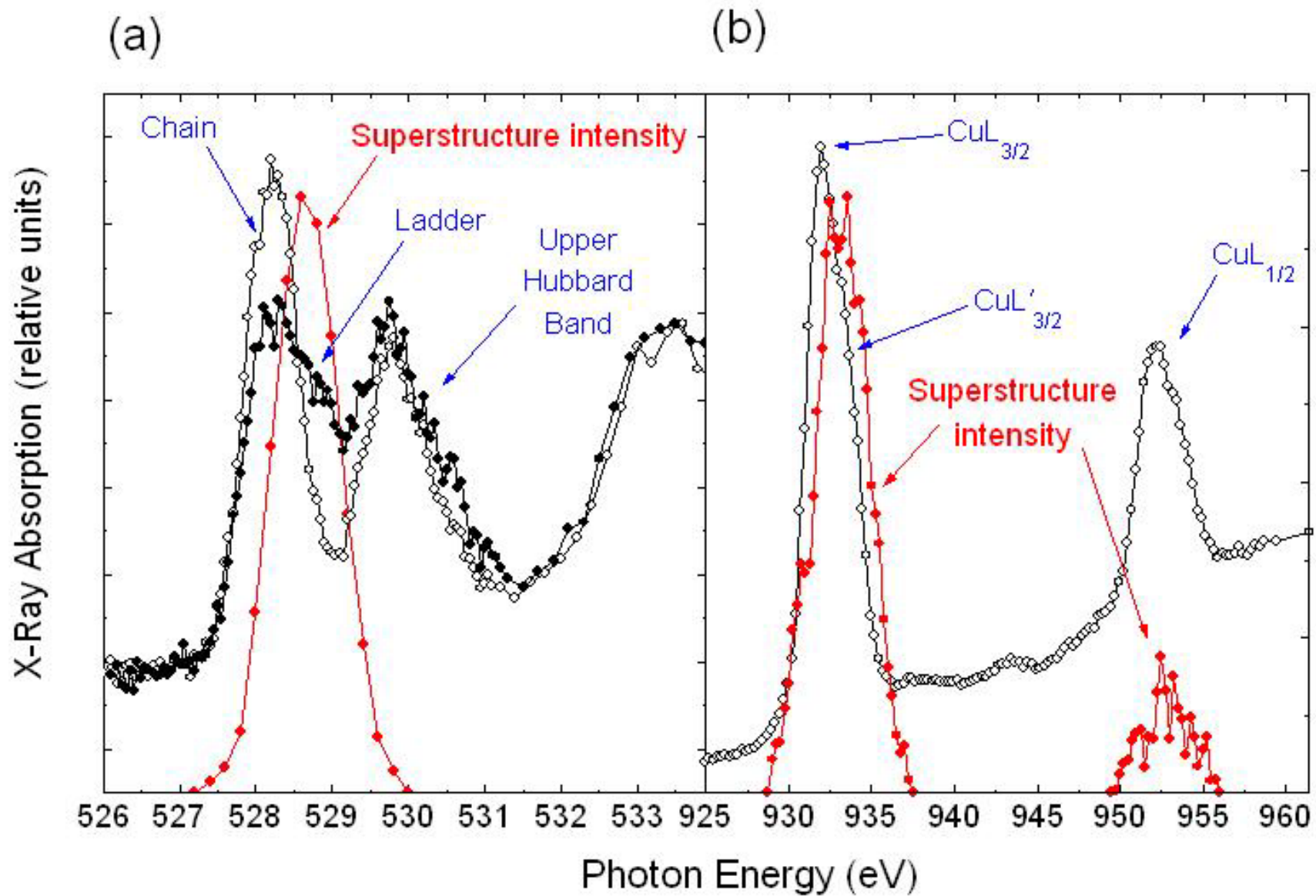
(a)

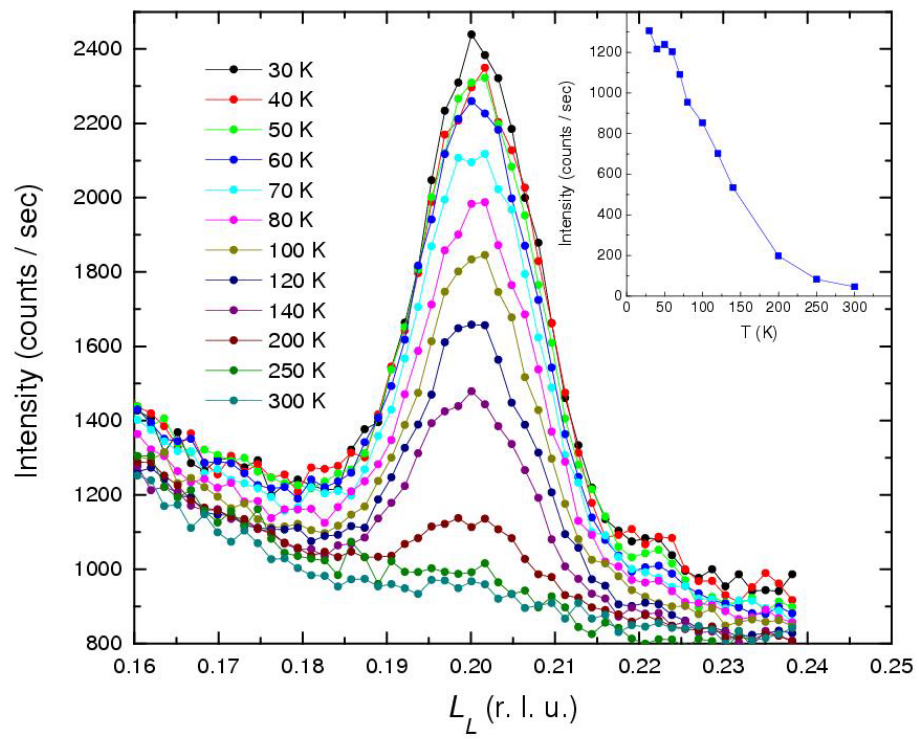


(b)

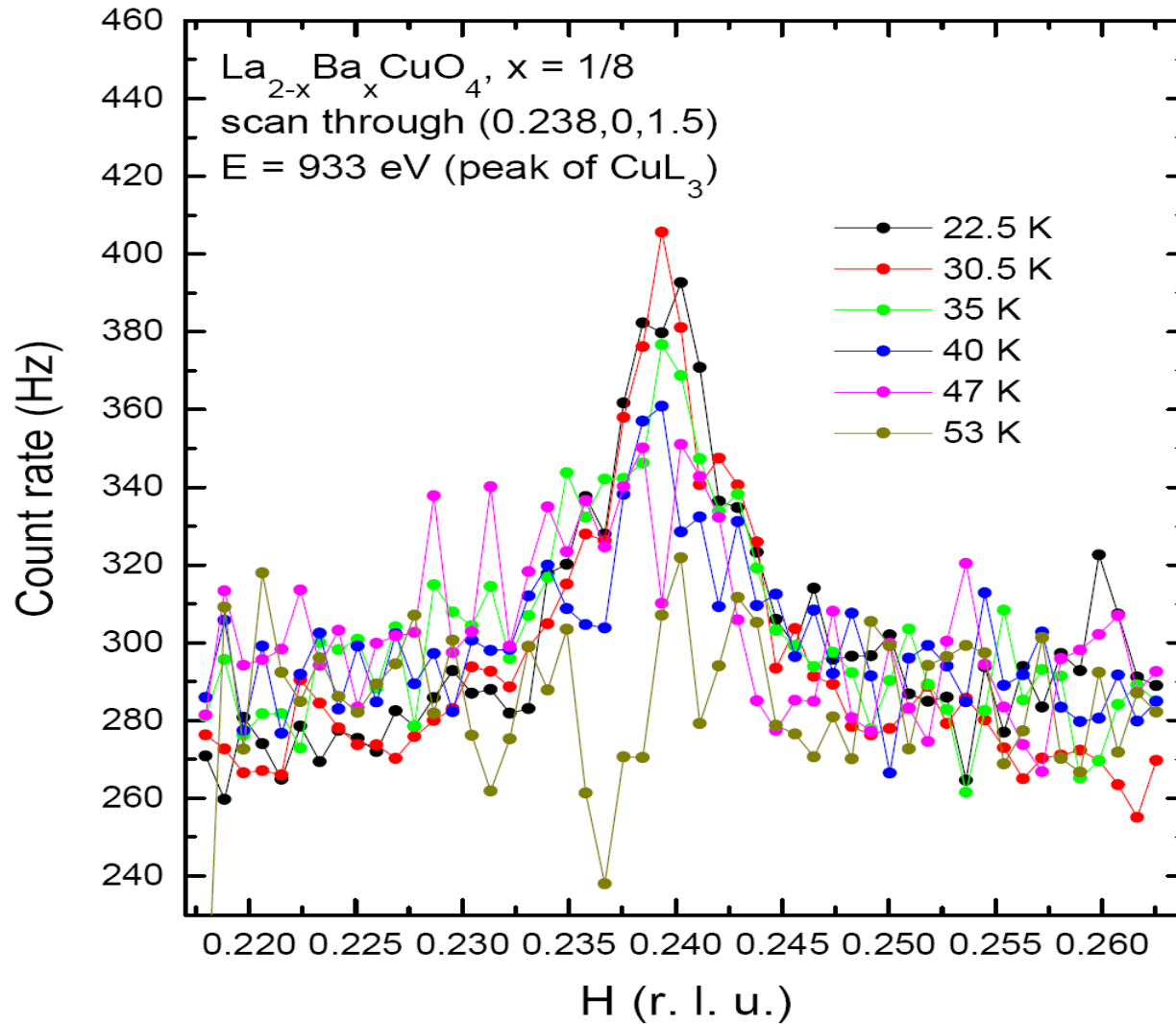


Photon Energy (eV)





Are there charge stripes in high T_c's ???



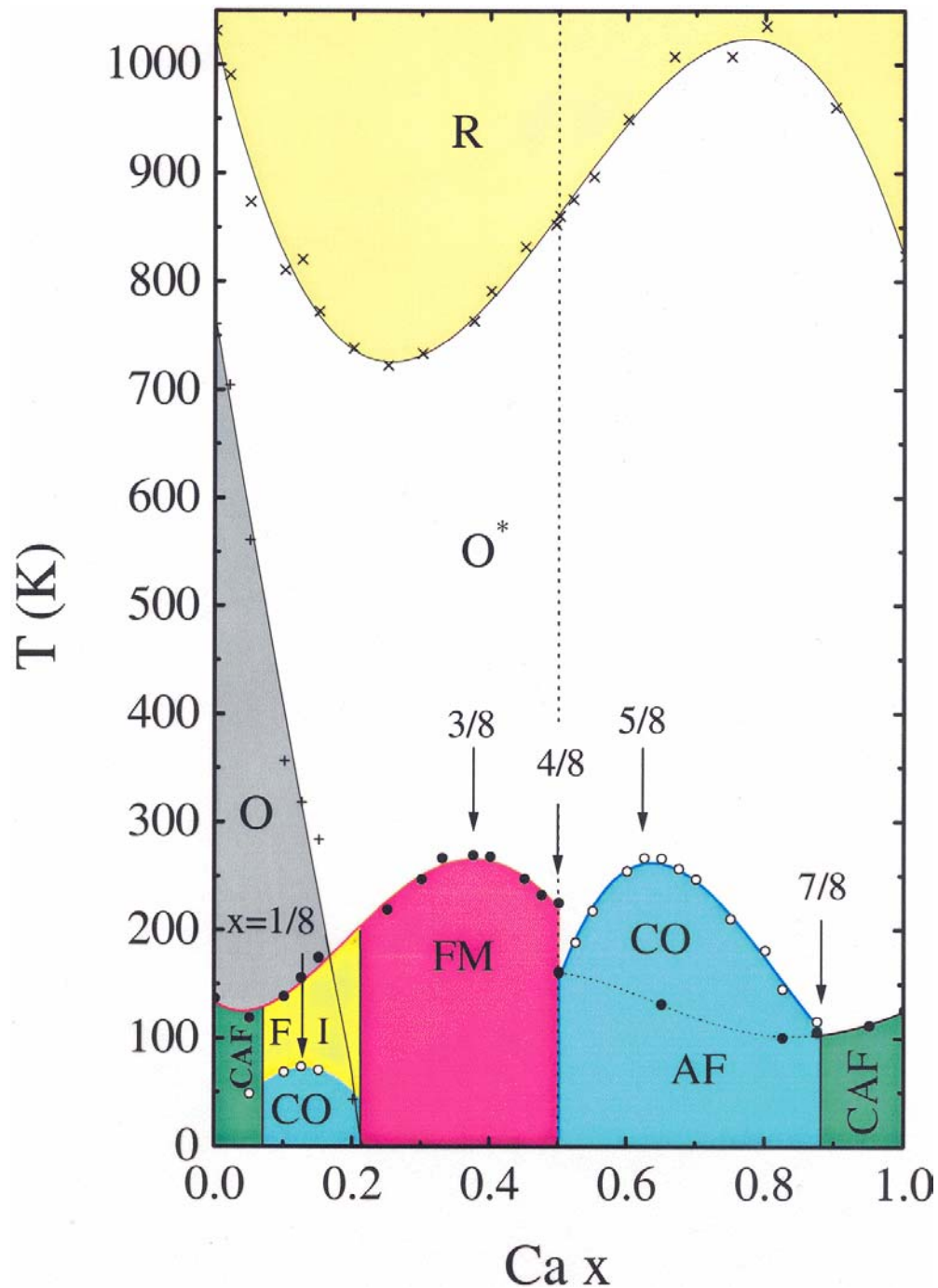
Phase Diagram of $\text{La}_{1-x}\text{Ca}_x\text{MnO}_3$

Uehara, Kim and Cheong

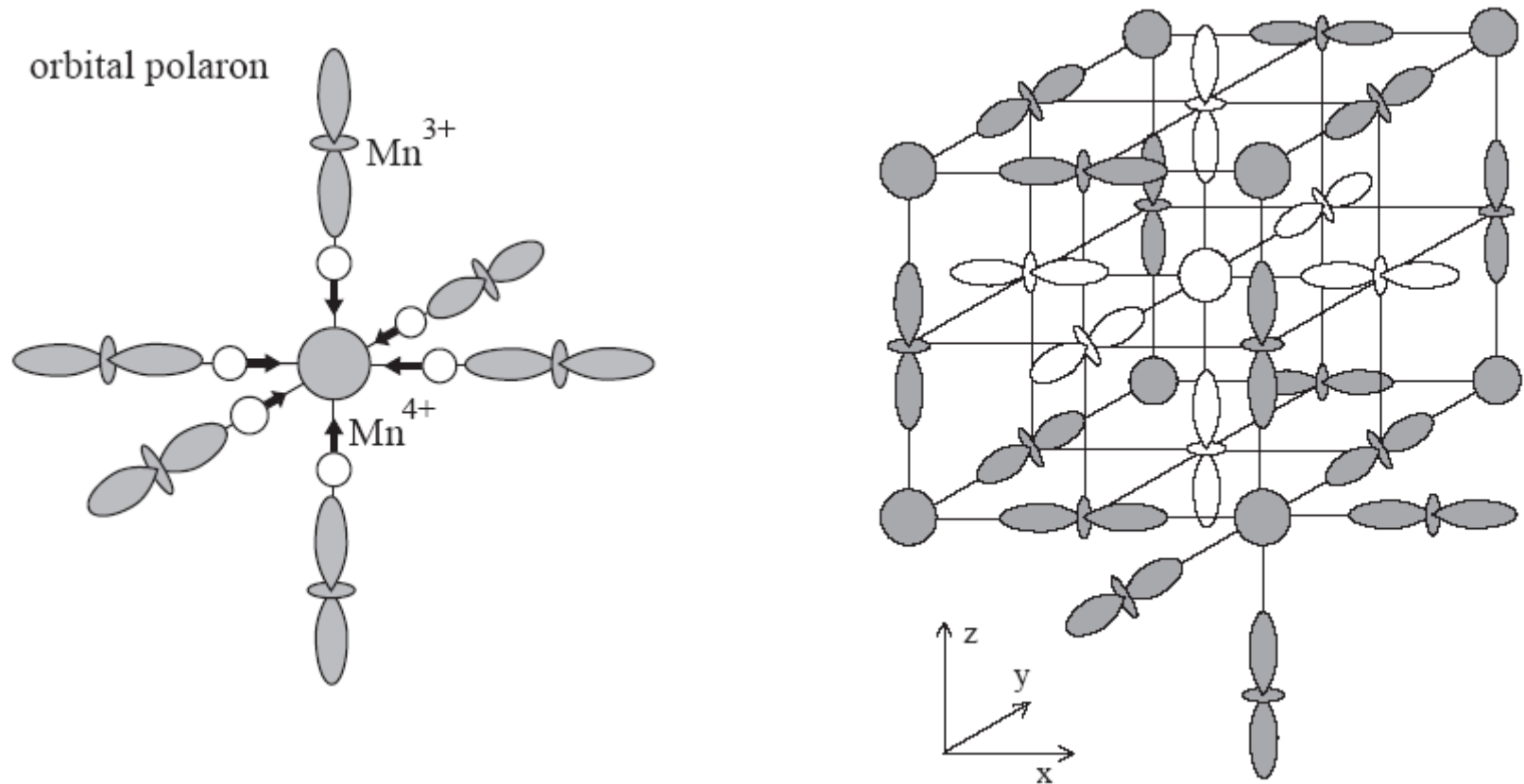
R: Rhombohedral

O: Orthorhombic
(Jahn-Teller distorted)

O*: Orthorhombic
(Octahedron rotated)



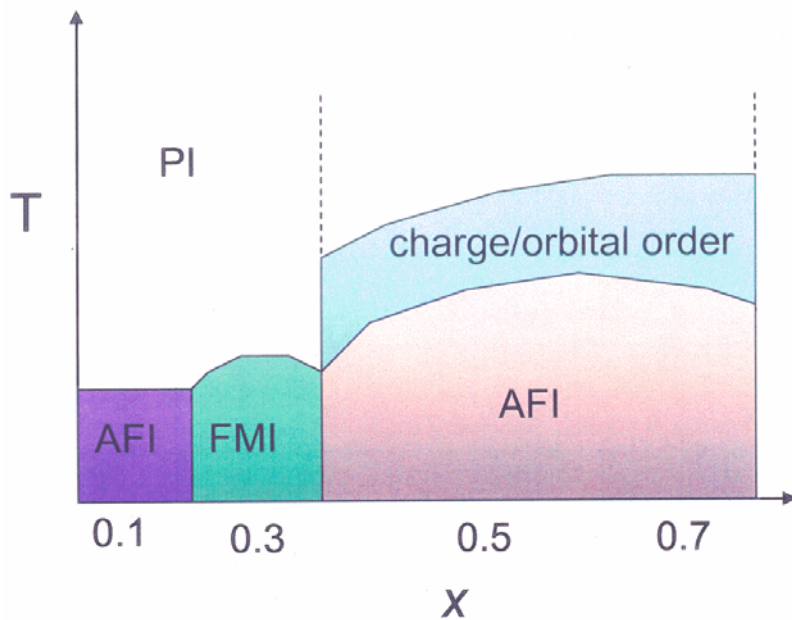
Model for Charge, Spin and Orbital Correlations in Manganites



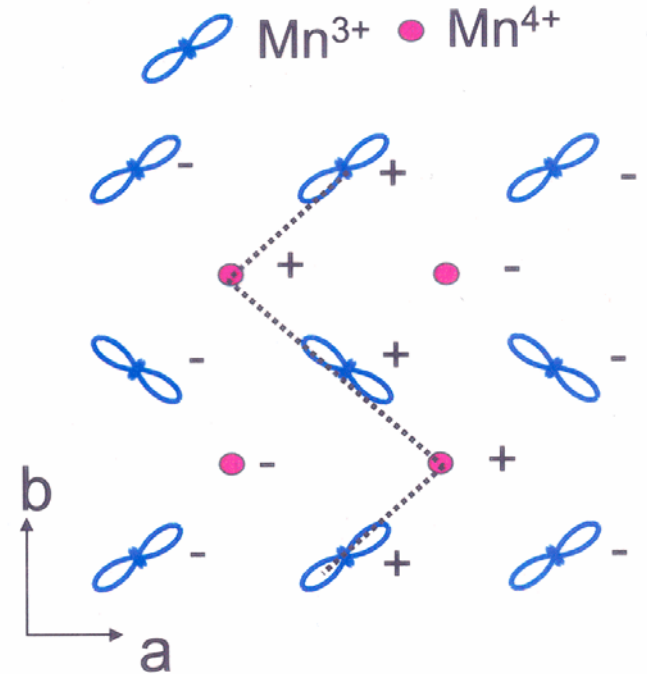
Mizokawa et al (2001)

$Pr_{1-x}Ca_xMnO_3$

$Pr_{0.6}Ca_{0.4}MnO_3$ CE type charge, orbital and magnetic order

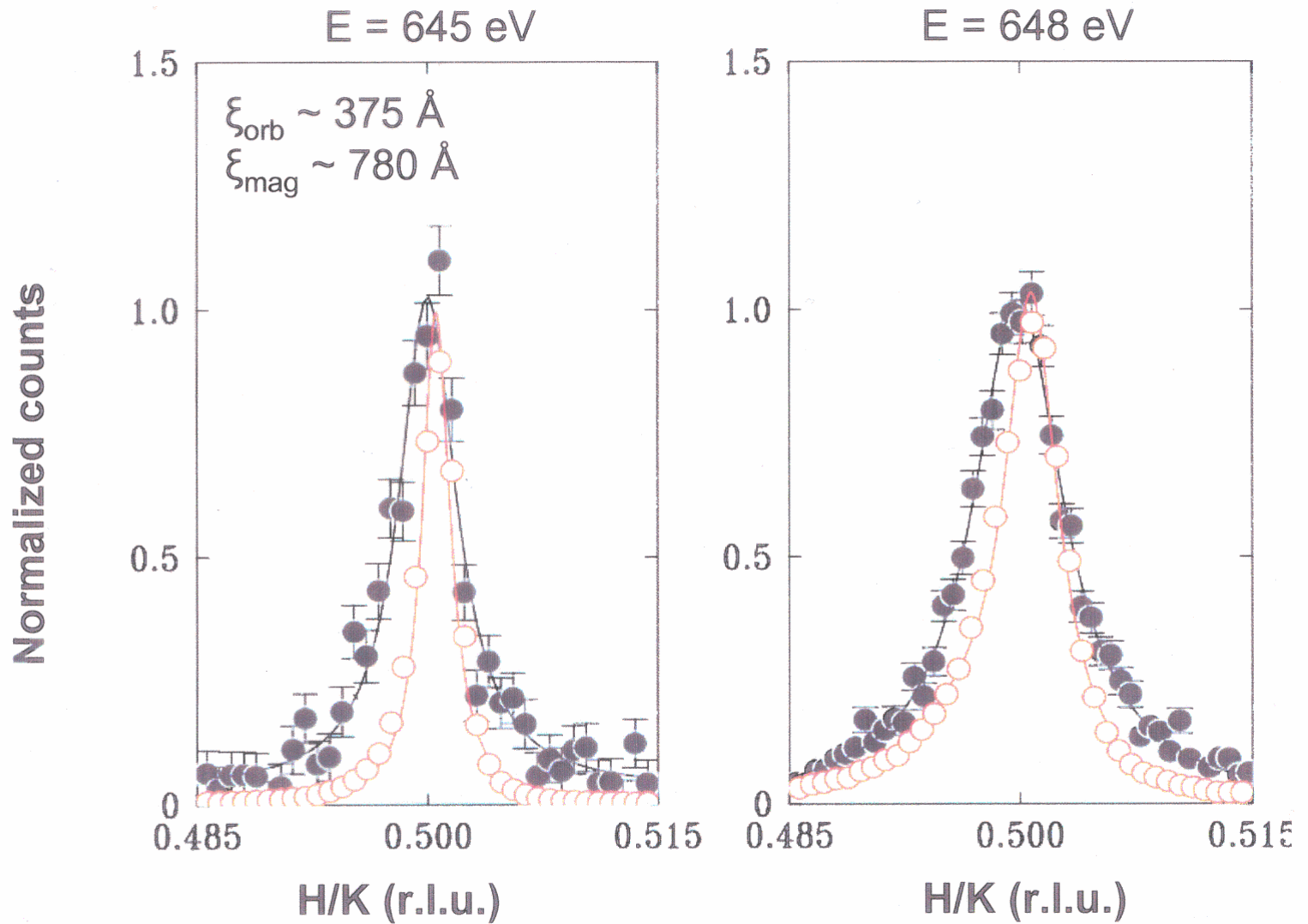


Goodenough (1955)

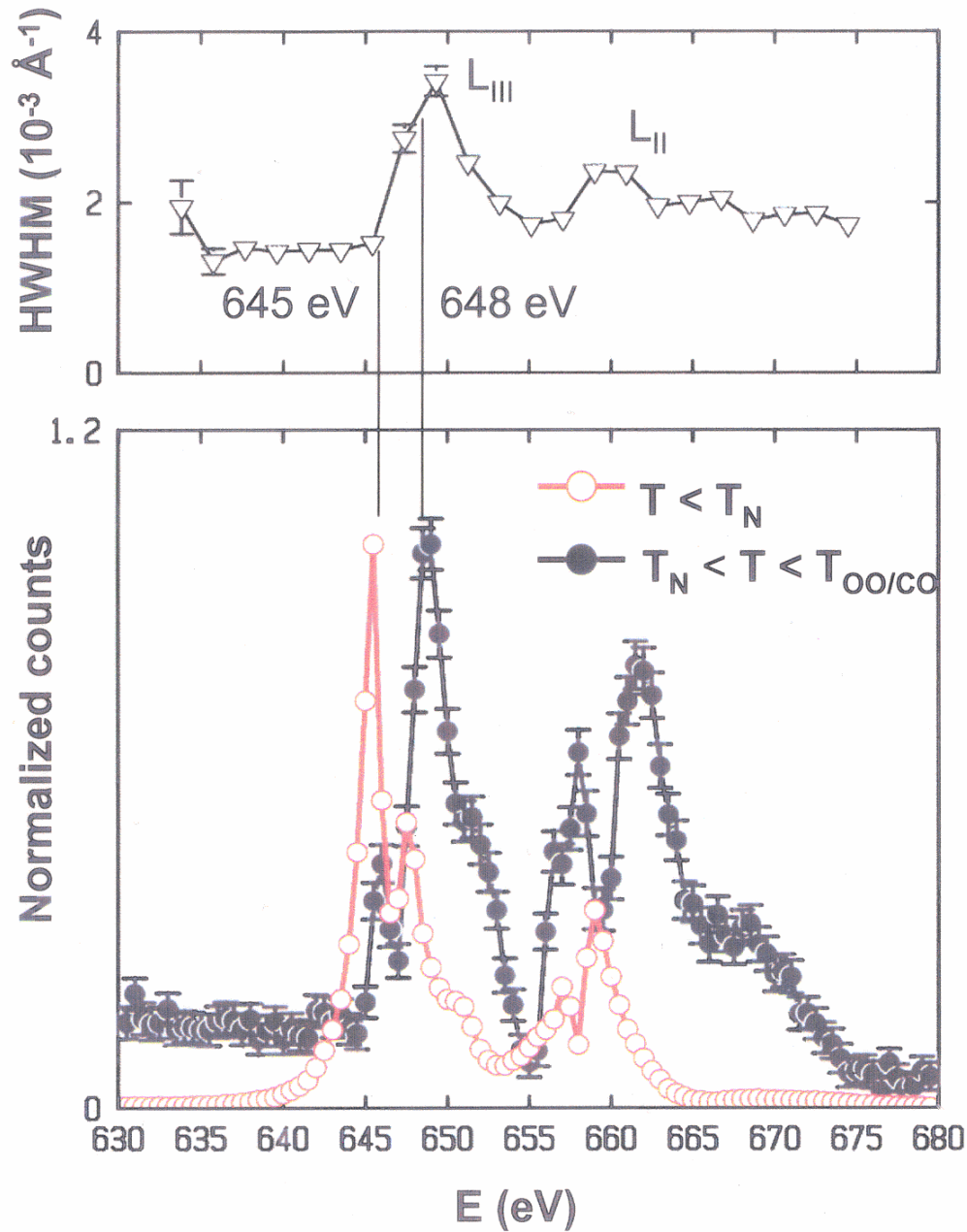


- Charge ordering below $T_{CO} \sim 240K$
- Cooperative orbital ordering + oxygen distortion at $T_{OO} = T_{CO}$
- Magnetic ordering below $T_N \sim 170K$

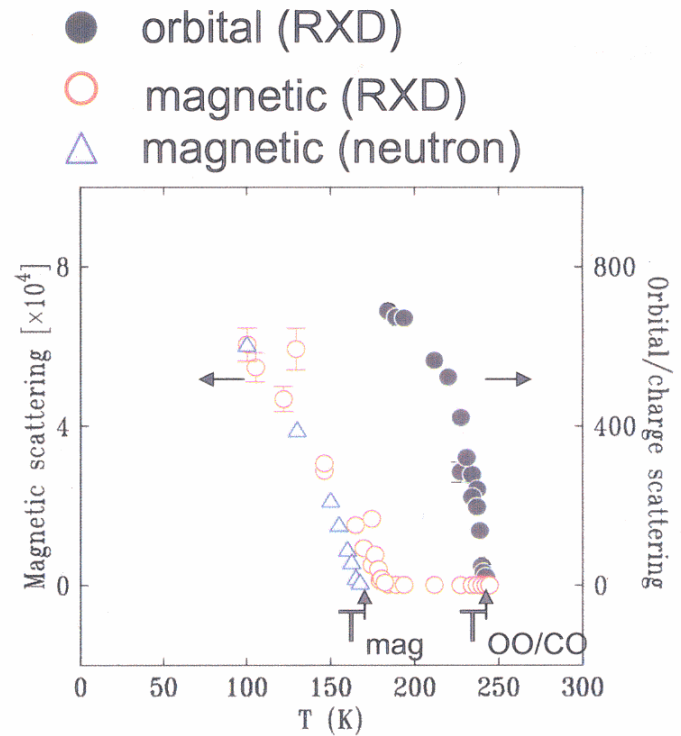
Longitudinal scans



- orbital scattering exhibits short range order



3 eV shift in spectral weight between the magnetic and orbital spectra



K.J. Thomas and J.P.Hill (2003)

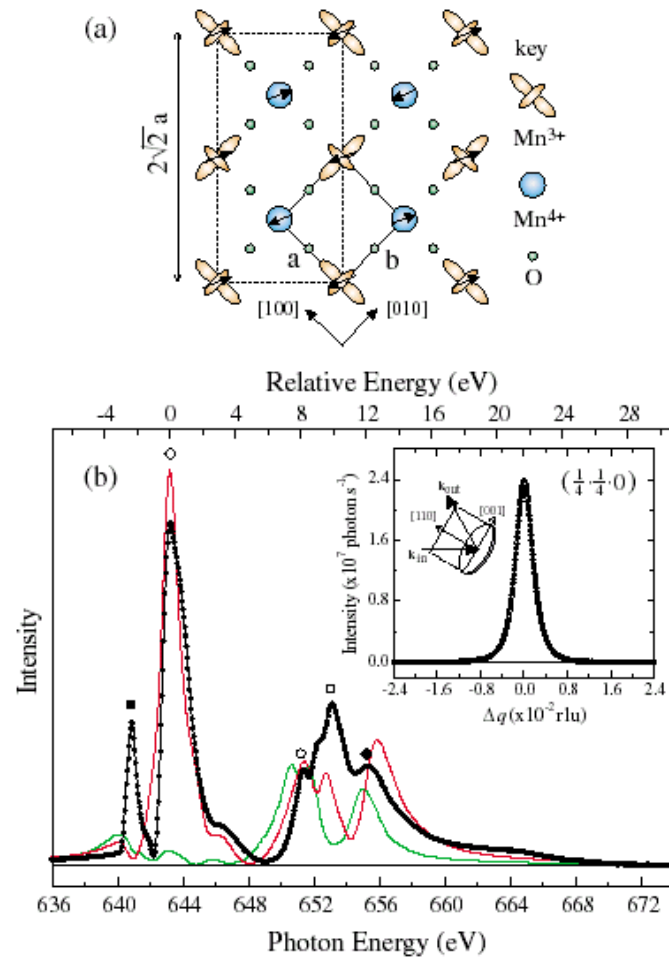
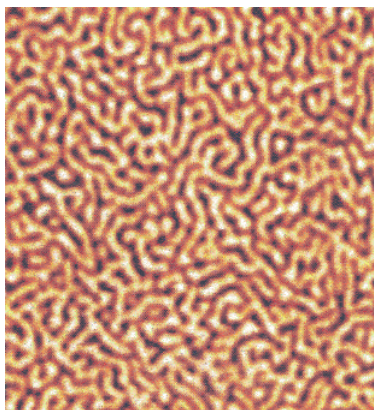


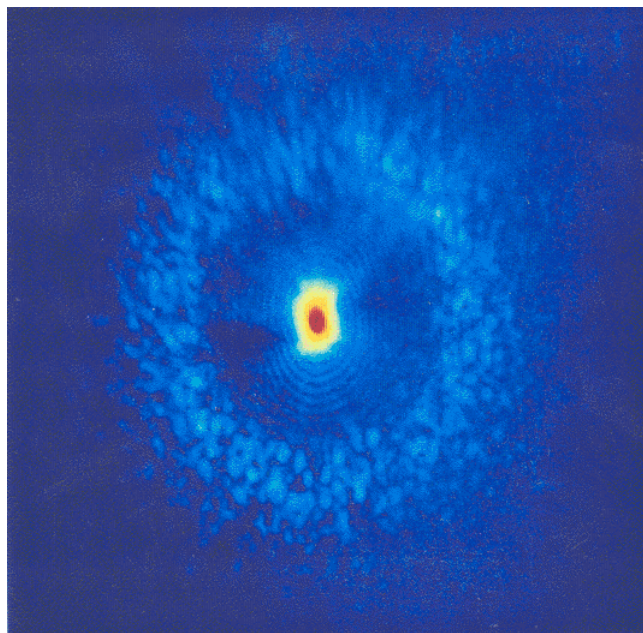
FIG. 1 (color). (a) Charge, orbital, and spin ordering in the MnO_2 planes of $\text{La}_{0.5}\text{Sr}_{1.5}\text{MnO}_4$; the arrows represent the magnetic moments. The primitive $I4/mmm$ unit cell is shown by the solid line ($a = b = 3.864 \text{ \AA}$) and the OO unit cell by the dashed line. (b) The energy dependence (solid circles with line) of the $(\frac{1}{4}, \frac{1}{4}, 0)$ peak recorded over the Mn $L_{2,3}$ edges at 134 K and the calculated spectrum in D_{2h} symmetry for large (red line) and small (green line) JTD. The inset shows a $(\frac{1}{4} + \Delta q, \frac{1}{4} + \Delta q, 0)$ scan of the forbidden reflection arising from OO at a photon energy of 643.8 eV and at $T = 134 \text{ K}$ (open circles). The solid line is a Lorentzian fit to the peak. The experimental geometry is also shown.

Coherent Soft X-ray Scattering

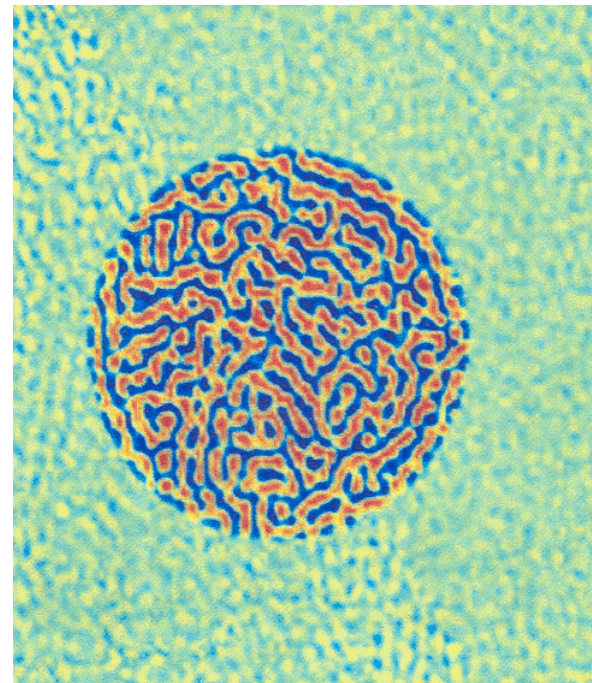
Magnetic
“Worm”
Domains



X-ray Speckle Pattern



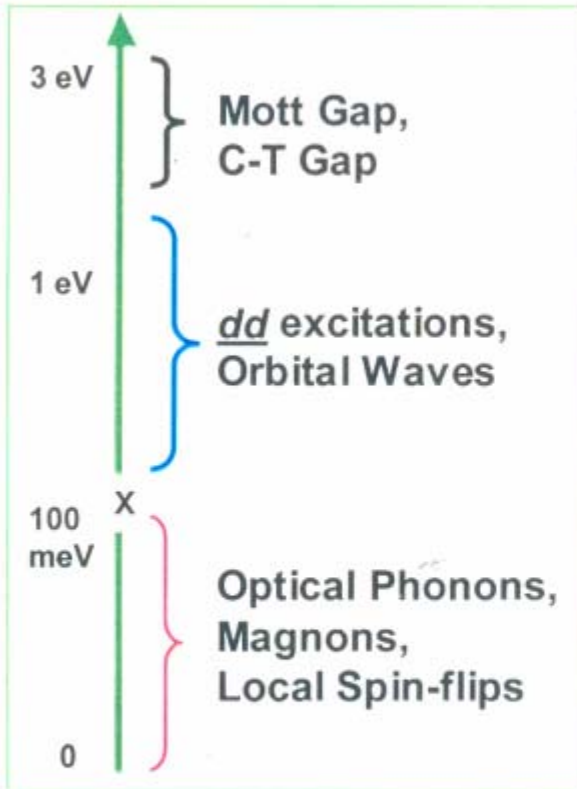
Domain Reconstruction



Example of a New Collaboration:

- oxide thin films, correlated electrons, nanomagnetism, electron spectroscopy
- UBC, SFU, FZ – Juelich, IBM Almaden, Stanford University, BESSY

Energy scales of various excitations



- Optical Phonons: ~ 40-70 meV
- Magnons: ~ 10 meV to 40 meV
- Orbital fluctuations (originated from optically forbidden **d-d** excitations): ~ 100 meV to 1.5 eV

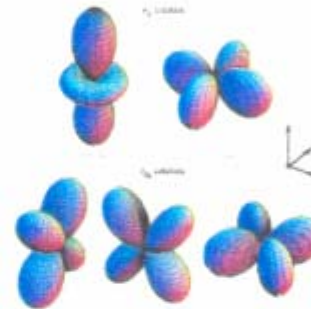
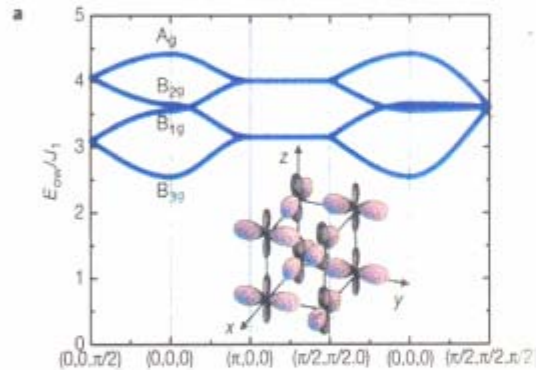
Understanding of interaction among the degrees of freedom at these energy scales requires study of energy losses up to ~ 3 eV (Mott-Hubbard edge) with energy resolution better than 10meV

Soft x-ray resonances (3p → 3d) provide the most sensitive channels of excitations to study **orbital wave excitations** (in addition to charge and spin excitations)

Orbital Degrees of Freedom

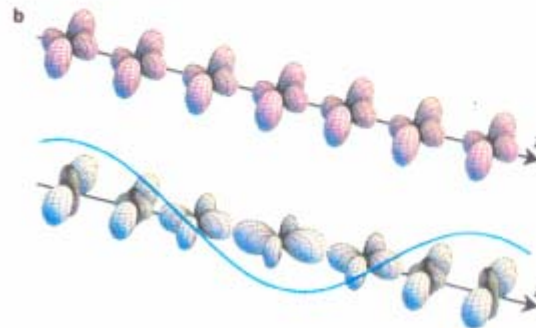


Ferromagnetic and AFM Mott Insulators



3d-Orbitals

Orbital Excitations fundamentally originate from dd excitations



Orbital Order

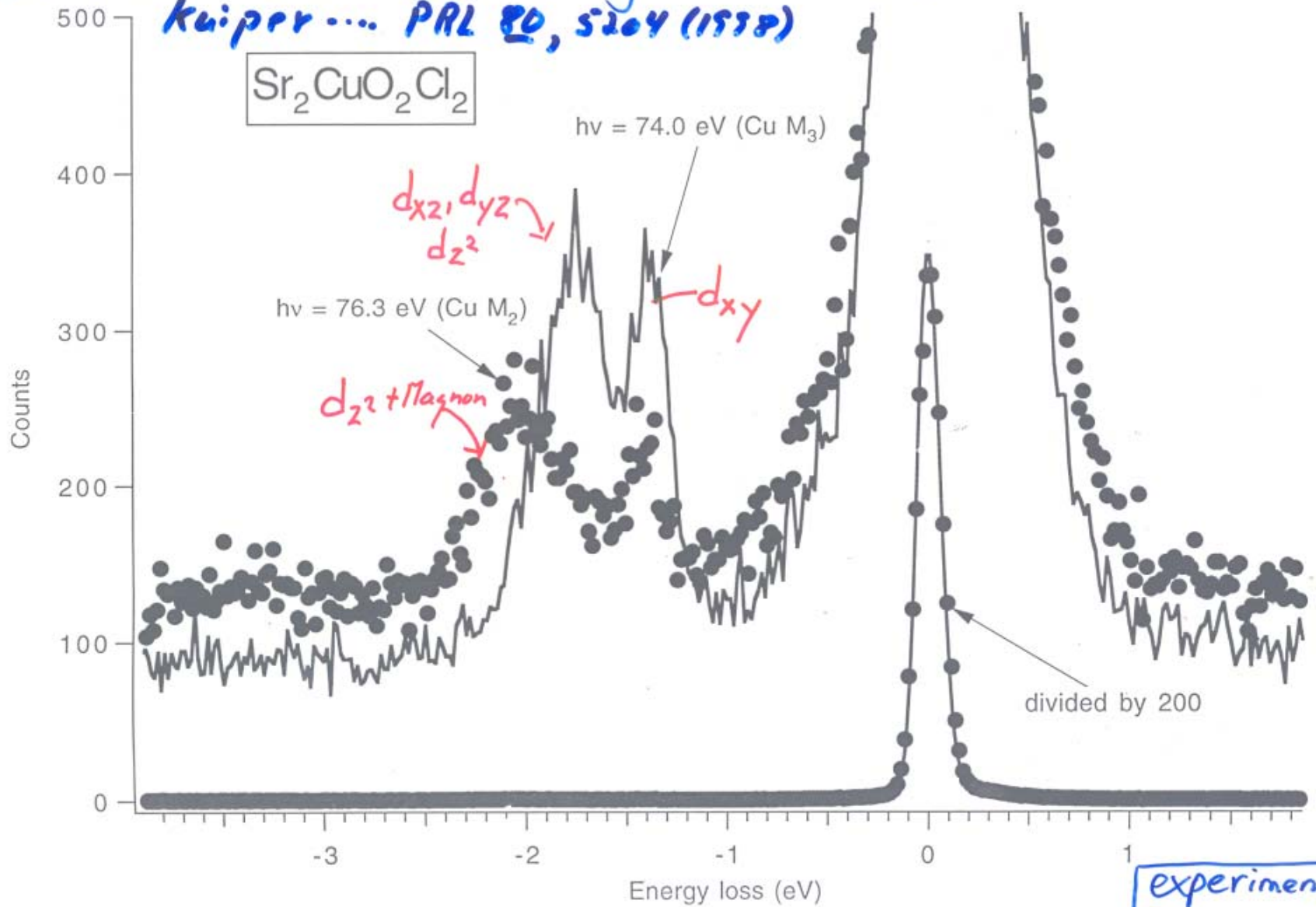
Orbital Excitations/"Orbitons"

Maekawa et al. (2001)

M.Z.Hasan (2002)

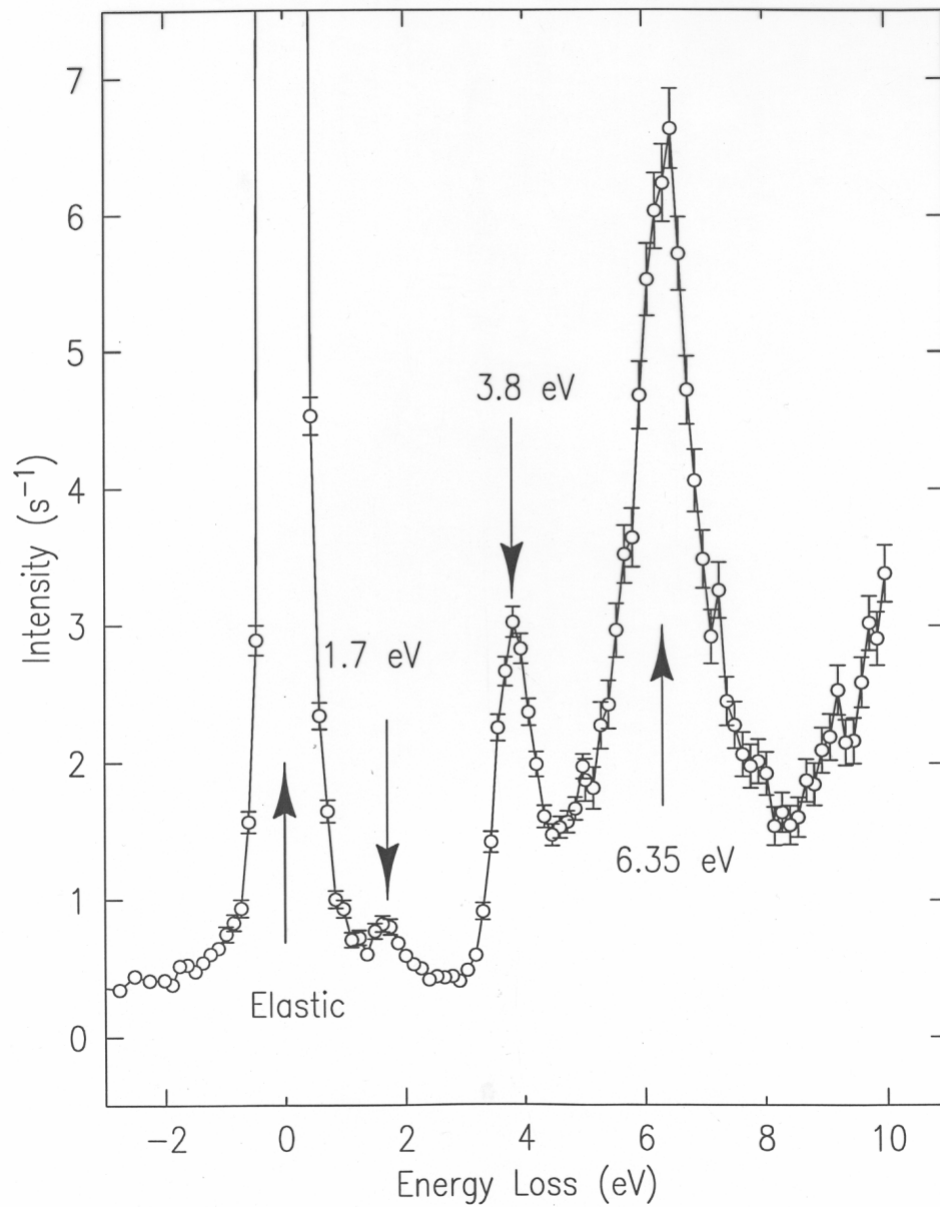
RESONANT INELASTIC X-RAY SCATTERING.

Kuiper ... PRL 80, 5204 (1998)



experiment:
P. Kuiper et. al.

CuGeO₃ Excitation Spectrum



Lattice of fluxoids ($H > H_{C1} < H_{C2}$)

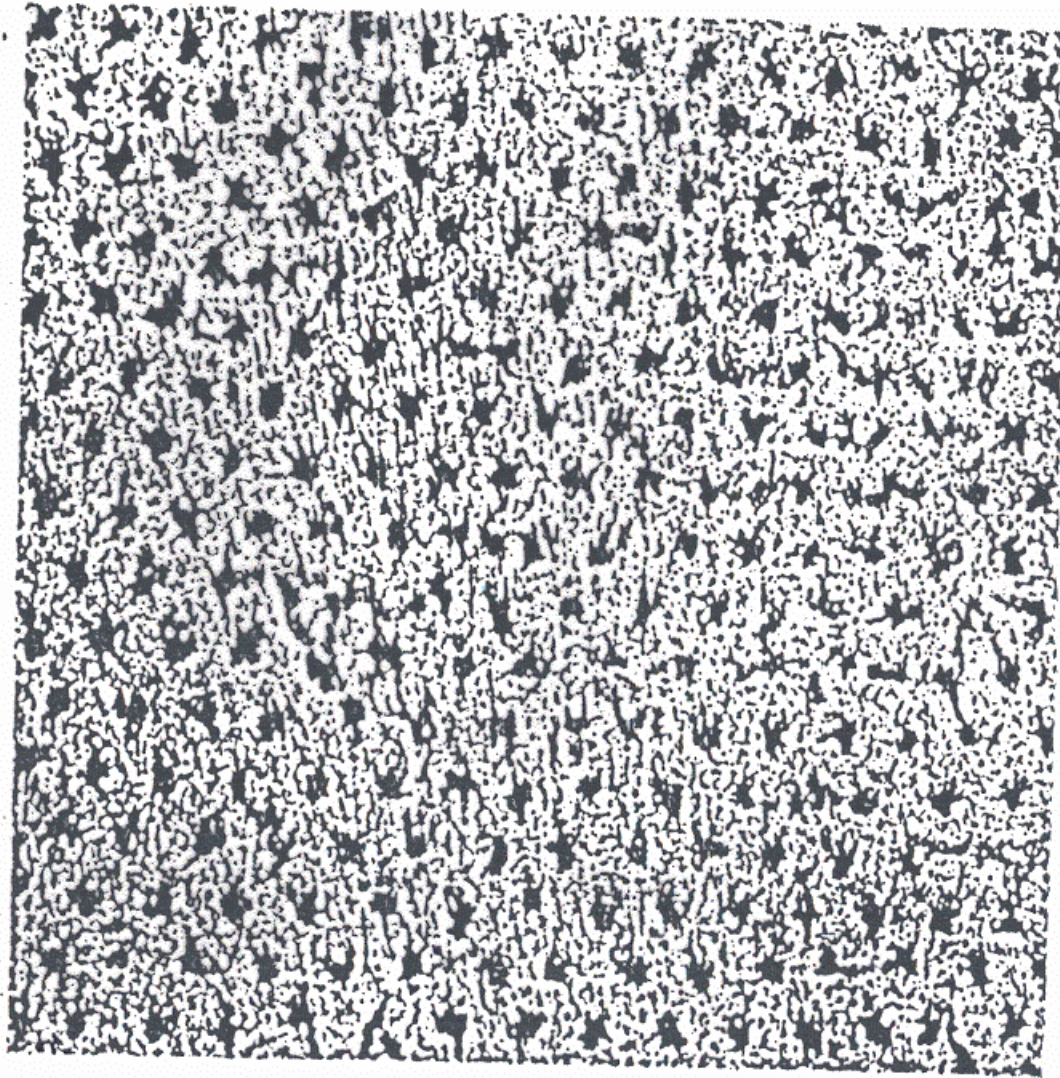


Figure 19 Triangular lattice of fluxoids through top surface of a superconducting cylinder. The points of exit of the flux lines are decorated with fine ferromagnetic particles. The electron microscope image is at a magnification of 8300, by U. Essmann and H. Träuble.

Vortex lattice of High T_C 's

Type II S.C.

$$a = 1.072 \sqrt{\frac{\phi_0}{B}} \quad \phi_0 = \frac{h}{2e}$$

10 Tesla \sim 100Å

Chemical potential for electrons $T < T_C$ changes by

$$\mu(T) = \mu_0 - \frac{\Delta^2(T)}{4\mu_0} \quad \mu_{S.C.} = \mu_{Npart} \quad i.e$$

μ of S.C. = μ of vortex core

• • Vortecies are charged

$$\delta n = \pi \xi^2 2N(\varepsilon_F) \delta \mu$$

For future studies we need:

- Circular polarized light
- Full polarization control [fast switching]
- Array of channelplate detectors or CCD
- Octopole superconducting magnet
- We will add two in-situ MBE systems for molecular and oxide ultra-thin film preparation
- Low Temperature

Near Future

1. Resonant X-ray Scattering

- Orbital Ordering
 - Charge Ordering
 - Spin Ordering
 - J.-T. Distortions
- } T, x, H dep.

2. Large length scales

(λ for 2p \rightarrow 3d in 3d TM \sim 15 Å)

- Vortex lattice in High T_C 's
- Charge and Spin density waves
- (Dynamic) phase separation
(stripes, puddles ...)
- Spatial distribution of selected organic groups
- Structure of organic blends – self assembly

3. Use of coherence

- Speckle – disordered systems

4. X-ray Raman

- electronic excitations
- Magnons
- Phonons
- Orbitons + Orbitoron \leftrightarrow Spin Wave
- q dependence

5. All the above in Microscopy

- focus to \sim 10 nm